ELSEVIER

Biochimica et Biophysica Acta 1513 (2001) 95–121

BIOCHIMICA ET BIOPHYSICA ACTA
BBA

www.bba-direct.com

Review

Slippage and uncoupling in P-type cation pumps; implications for energy transduction mechanisms and regulation of metabolism

Mervyn C. Berman *

Division of Chemical Pathology, Health Sciences Faculty, University of Cape Town, Observatory 7925, Cape Town, South Africa

Received 12 March 2001; received in revised form 8 May 2001; accepted 17 May 2001

Abstract

P-type ATPases couple scalar and vectorial events under optimized states. A number of procedures and conditions lead to uncoupling or slippage. A key branching point in the catalytic cycle is at the cation-bound form of E_1-P, where isomerization to E_2-P leads to coupled transport, and hydrolysis leads to uncoupled release of cations to the *cis* membrane surface. The phenomenon of slippage supports a channel model for active transport. Ability to occlude cations within the channel is essential for coupling. Uncoupling and slippage appear to be inherent properties of P-type cation pumps, and are significant contributors to standard metabolic rate. Heat production is favored in the uncoupled state. A number of disease conditions, include ageing, ischemia and cardiac failure, result in uncoupling of either the Ca^{2+}-ATPase or Na^+/K^+-ATPase. © 2001 Elsevier Science B.V. All rights reserved.

Keywords: P-type ATPase; Slippage; Uncoupling; Variable stoichiometry; Channel; Occluded cation; Partial denaturation; Heat production

1. Introduction

This review is ultimately concerned with mechanisms by which biological energy is interconverted. Energy transduction mechanisms have been the subject of intensive investigation since Mitchell first introduced his chemiosmotic hypothesis [1,2]. Whilst it is quite clear that scalar and vectorial reactions of ATP and protons are linked and interconvertable, this is one aspect of the original hypothesis that is least certain. Chemiosmotic principles are relevant to a wide variety of membrane-linked energetic phe-

Abbreviations: A23187, calcimycin; Ca^{2+}-ATPase, Ca^{2+}- and Mg^{2+}-activated adenosine 5′-triphosphatase (EC 3.6.1.38); Na^+/K^+-ATPase, Na^+- and K^+-activated adenosine 5′-triphosphatase (EC 3.6.1.37); SR, sarcoplasmic reticulum; E-P, phosphorylated forms of P-type ATPase; E_1-P, forms with high affinity cytosolic-orientated cation binding sites; E_2-P, forms with low affinity extracytosolic-orientated cation binding sites; TG, thapsigargin; TNP-ATP, 2′(3′)-*O*-(2,4,6-trinitrophenyl) adenosine-5′-triphosphate; $[Ca^{2+}]_{lim}$, limiting concentration of medium or cytosolic free calcium ions; EGTA, ethylene bis(oxyethylene nitrilo) tetraacetic acid; DMSO, dimethylsulfoxide; CPA, cyclopiazonic acid; HCPL, high cholesterol proteoliposomes; LCPL, low cholesterol proteoliposomes; NEM, *n*-methylmaleimide; MGS, molten globular state; SDM, site-directed mutagenesis; SMR, standard metabolic rate; NST, non-shivering thermogenesis; SERCA, sarco- and endoplasmic reticulum Ca^{2+}-ATPase; GABA, γ-aminobutyric acid; $K_{0.5}$, concentration at half maximal effect; DOPC, dioleoylphosphatidylcholine; AcP, acetylphosphate

* Fax: +27-21-4488150. *E-mail address:* mervyn@chempath.uct.ac.za (Mervyn C. Berman).

0005-2736/01/$ – see front matter © 2001 Elsevier Science B.V. All rights reserved.
PII: S0005-2736(01)00356-X

nomena, including oxidative phosphorylation, regulation of cell volume and membrane potential, secondary solute cotransport and transepithelial fluxes of water and salts. Although intermediate reactions of such systems have been particularly well investigated, we are still uncertain as to how chemical and vectorial processes are linked. The P-type Na/K- and Ca-ATPases, together with the light-driven H^+ pump, bacteriorhodopsin, appear to be the most promising systems with which to understand transduction mechanisms. Here we will consider the evidence for fixed and variable stoichiometry or uncoupling in the P-type ATPases. We will also discuss what mechanistic implications are at stake, and the physiological and pathological issues that are involved.

The relaxing factor present in mitochondrial supernatant homogenates of skeletal muscle was identified independently in 1963 by Ebashi and Lippman [3], and by Hasselbach and Makinose [4], as the Ca^{2+}-transporting and -dependent membrane-bound Ca^{2+}-ATPase that utilizes energy of ATP hydrolysis, coupled to ion translocation against a concentration gradient, to lower cytosolic [Ca^{2+}] into the submicromolar range. Ebashi and Lippman noted that preparations of sarcoplasmic reticulum (SR) vesicles lost their ability to transport Ca^{2+} on storage, whilst ATPase activity was either unaffected or even enhanced. They suggested that the Ca^{2+} pump mechanism might become uncoupled with ageing. This question remains a key issue and this review focuses on recent evidence, which indicates that uncoupling or slippage is a characteristic feature of P-type cation pumps.

According to the E_1/E_2 model, shown in Fig. 1, P-type ATPases are phosphorylated by ATP, which simultaneously alters the orientation and affinity of cation transport sites in a highly coordinated manner, leading to uphill transfer against a 10^4:1 concentration gradient in the case of the Ca^{2+}-ATPase, 10:1 for the Na^+/K^+-ATPase and 10^5:1 for the gastric H^+/K^+-ATPase. The question we seek to answer is whether turnover is obligatorily tightly coupled to ion transport, or whether these processes are able to occur independently, in which case the system is said to 'slip', or to be uncoupled. If such behavior is confirmed this should enable us to favor one or more of the current models.

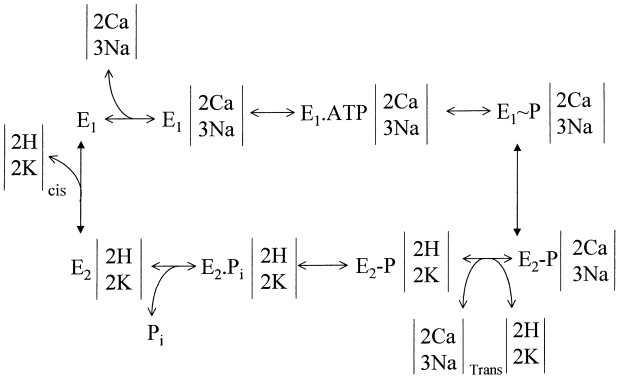

Fig. 1. Catalytic cycles of the Ca^{2+}-ATPase and Na^+/K^+-ATPase. '*Cis*' refers to the cytosolic membrane surface. 'Trans' is to the SR lumen and extracellular surfaces respectively.

Reaction cycles, based on the original de Meis and Vianna unbranched model for the Ca^{2+}-ATPase [5], implied tight coupling with fixed Ca^{2+}/ATP ratios of 2.0 over wide ranges of solute concentrations. Similarly, the ratio of Na^+:K^+:ATP of 3:2:1 is predicted by the Post–Albers scheme, as modified by Karlish for the Na^+/K^+-ATPase [6]. Tight coupling can be achieved by the alternating access model formalized by Tanford [7] (Fig. 2A). A different mechanism is based on channel-like properties of the pump, according to the model first proposed by Lauger [8]. In the latter case, conformational events are coupled to steps in the reaction cycle that lead to gating and synchronous waves of change in energy barrier heights between in-line or serial cation binding sites within the channel (Fig. 2C). Such a process would be expected to behave stochastically, and be compatible with a wide range of coupling ratios, depending on reaction conditions. Various terms with different implications have been used to describe this phenomenon, including variable coupling ratio, variable stoichiometry, uncoupling or slippage. These are discussed in more detail in Section 2.

The E_1/E_2 model and its various derivatives all presume that the transported ions remain bound to their initial sites during the pump cycle, and that access and affinity alternate between outward facing high affinity, and inward facing low affinity sites. The alternate 'channel' hypothesis is that ions move/jump from fixed sites on opposite sides of the membrane with appropriate accessabilities and affinities.

Skeletal muscle SR is highly differentiated. Its only

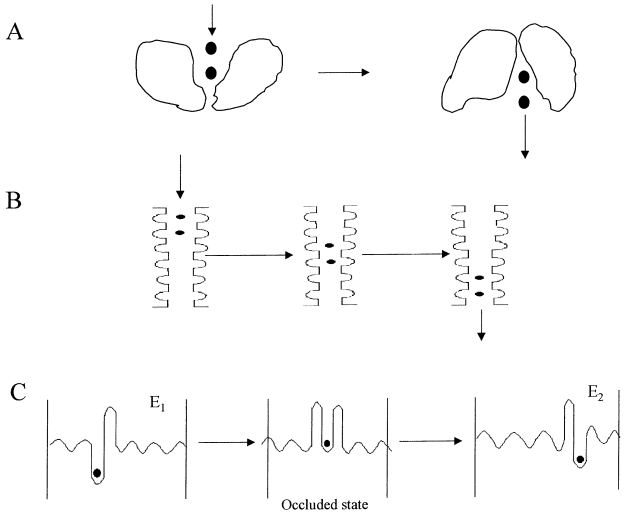

Fig. 2. Mechanistic models of active cation transport. A: Alternating access; B: fixed channel; C: energy barrier model (Lauger, [19]).

functions appear to be uptake of sarcoplasmic Ca^{2+}, mainly confined to the cisternal location, resulting in muscle relaxation, and release of Ca^{2+} via ryanodine-sensitive channels located in terminal cisternae, where physical apposition to T-tubules enables plasma membrane depolarization to be linked to Ca^{2+} release through 'foot' structures in the triadic junction. The magnitudes of Ca^{2+} fluxes during contraction and relaxation are considerable, with maximum currents equivalent to 8 and 0.8 amps/gm during contraction and relaxation respectively [9]. This accounts for high ATP consumption of approximately one-third of total energy consumption during muscular activity.

According to current understanding there remain unanswered questions regarding coupling and uncoupling mechanisms. One major aim of this review has been to examine those conditions that lead to apparent uncoupling and the nature of the uncoupled state.

1.1. Channels and carriers

The basic differences between channel and alternating access mechanisms of membrane transport are readily appreciated by their characteristic properties. Channels are presumed to have a fixed conformation, and have high non-saturable conductance rates (>100–$1000\ s^{-1}$) with no competition between transported species on both *cis* and *trans* membrane surfaces. Carriers on the other hand, which are the basis for alternating access, do undergo conformational changes on binding of ligands, their movement or accessibility across the membrane limits transport rate ($<10\ s^{-1}$), and binding of ligands is competitive and interactive. Stoichiometries of ligand binding are fixed in the case of carriers, but are independent and meaningless for channels. The experimental findings of variable coupling ratios and slippage favor a channel-like mechanism. We should note also that carrier-like properties can be described in channel structures in terms of controlled 'gates' and energy barriers.

Early descriptions of membrane transport invoked a shuttle mechanism in which a carrier moves within the confines of the membrane and alternately exposes ligand binding sites to either membrane surface. Later, when the physical nature of transporters became apparent, with sizes in the 100 kDa range, and hydrophobic interactions with surrounding membrane lipids were characterized, it became obvious that physical movement of the transport protein within the membrane was highly unlikely. This resulted in early proposals by Patlak [10], Vidavar [11] and Jardetzsky [12] of fixed allosteric models, and later descriptions of the alternating access model by Dutton et al. [13], Lauger [8], Klingenberg [14], Kyte [15] and Tanford [7]. The standard representation shows a set of localized cation binding sites with jaw-like opening and closing of wide funnels connecting the sites alternately to opposing membrane surfaces (Fig. 2A). During active transport access of ions to the binding site is alternated by the energy source involving conformational changes such that energy barrier heights are manipulated with resultant release of ions up a concentration gradient. Tanford [16] has explained this in terms of twisting and tilting of adjacent intramembranous helices, whose side chains share in the cation binding process. It can be inferred from their size that transport sites only occupy a fraction of the total transmembrane distance, which leads to the idea that access channels must provide a path to both membrane surfaces. Jennings [17] has defined an access channel as a pathway for ion diffusion that does not depend on conformational changes of the energy transducing transport protein. Access pathways corresponding to this definition have

been described in the Na/K-ATPase [18] and erythrocyte anion translocator [17]. Lauger [19] has set two limiting cases for the access channel:

1. Low field access channels having nearly unrestricted access to the medium, with high conductance and low voltage drop, and
2. High field access channels, with restricted size and access to medium, and consequent low conductance, where a significant fraction of transmembrane voltage drops over its length, so that the apparent affinity of the transport site is voltage-dependent. The ion well postulated for proton access to the ATP synthase of mitochondria by Mitchell and Moyle [20] conforms to this high field type, and was originally proposed on the basis of kinetic equivalence of H^+ and of potential gradients during oxidative and photophosphorylation. The idea of a channel-like structure for energy transducing ATPases is therefore not novel.

The potential profile of an ion, crossing the membrane via a channel-like path (Fig. 2C), has been discussed by Lauger [19]. Two conformations, HE′-P and E″-P, with and without bound H^+, are phosphorylated states of an ATP-driven proton pump. The total voltage across the membrane, V, is partitioned between ion wells. If α' and α'' are the distances between wells and membrane surfaces, and β is the width of the energy barrier, then the dielectric distances $\alpha'+\alpha''+\beta=1$. If α' and α'' are positive, the affinities of the two phosphorylated states, $1/K'$ and $1/K''$, are voltage-dependent. During the conformational transition, HE′-P → E″-P, the ion is translocated over a distance with relative dielectric distance β, together with its ligand sphere [19]. Of special interest for current models of active ion transport is the case, discussed by Slayman and Sanders [21], in which β is very large without any physical movement of the ion, and $\alpha'=\alpha''=0$. This means that the access channels are low field, and the field moves past the stationary ion, and closes one access pathway whilst opening the opposing one, which is identical to the alternating access mechanism, considered above. We see, therefore, that alternating access is the extreme case of a channel-like mechanism.

Lauger, in 1979 [8], proposed a channel mechanism for electrogenic ion pumps (Fig. 2C). The essential features of this model are that the channel consists of a sequence of multiple binding sites of minimal energy, separated by activation-energy barriers, which span the thickness of the membrane, similar to that proposed for passive ion transport. Lauger applied this 'barrier' channel model to the proton pumping action of *Halobacterium* and to redox-driven proton pumps, and also suggested that similar considerations might apply to ATP-driven ion pumps, where minor conformational changes could alter dipolar moments of side chains involved in binding of the ion within the channel [8]. The channel model does not require alternating access or gates and is cast in a more general framework.

In the alternating access model there are a definite series of transitions during each successive pump cycle, with return to the starting intermediate state. The major difference in the proposed channel/single file mechanism is that there is no cycle, but a continuum of states, rather like the movements of a 'caterpillar'. Su et al. [22] have recently proposed a multi-substrate single file model for ion-coupled transport. The model includes single file arrangement of two substrates in a channel with multiple sites. 'Hopping' between sites, their frequency, and the effects of external voltage and attraction/repulsion between ligands, are included in the model. An analysis of a simple three-site model resulted in a 'hopping' diagram, consisting of 26 non-identical substates, based on site occupancy. Simulation of GAT1, a γ-aminobutyric acid (GABA)/Na^+ transporter, showed two major transport cycles that operate simultaneously. One cycle releases Na^+ alone, whilst the other both Na^+ and GABA together. Variable partition of fluxes between these two cycles could explain the observed substrate flux ratios ($1 < Na^+/GABA < 2$) with varying substrate concentration and external voltage. The model closely predicts behavior of the Na^+/GABA system. The depicted 'pockets' need not be physical recesses. Rather, attractive and repulsive motions of side chains of 5 Å could form energy pockets, separated by energy barriers. This contrasts with global protein conformational changes inherent in the E_1/E_2 alternating access models.

Addition of millimolar Ca^{2+} to skinned muscle preparations results in formation of blebs or 'sarcoballs' as described by Stein and Palade [23]. These arise from cisternal SR that is rich in Ca^{2+}-ATPase

units; approximately 20 000 pump units per μm^2. Wang et al. [24] have characterized the ion specificity and sensitivity to inhibitors of the Ca^{2+}-ATPase, and of the ryanodine-sensitive Ca^{2+} release channel, of blebs of SR, by the patch clamp technique. Calcium selective channels have three conductance states, α, β and γ of 70 ps, 50 ps and 37 ps, of which the β state predominates. Open probabilities of the channel were insensitive to ryanodine, ruthenium red, and also unaffected by millimolar ATP, Mg^{2+}, caffeine and Ca^{2+}, which is unlike the physiological Ca^{2+} release channel of terminal cisternae. However, Ca^{2+} conducting channels were sensitive to inhibitors of the Ca^{2+}-ATPase, including vanadate, AlF^{4-}, reactive red 120 and cyclopiazonic acid, implying that these channels were some form of the Ca^{2+} pump.

Such behavior could be attributed to a channel within the Ca^{2+}-ATPase that is open or unoccluded for 0.005% of the time. This mode of action of the Ca^{2+} pump may be due to loss of coupling to the transport cycle, with the result that it is turned into a Ca^{2+} conductance channel [25]. The Ca^{2+}-ATPase confers considerable Ca^{2+} permeability to SR membranes [26,27]. Several mechanisms could account for channel-like behavior of SR, including reversal of Ca^{2+}-ATPase activity, partial reactions of the catalytic cycle, or the Ca^{2+}-ATPase acting as a carrier. One favored explanation is that the channel is a rare conformation of the Ca^{2+}-ATPase, containing an open unoccluded state. However, the relevance to the pump cycle is as yet uncertain [24], and the nature of the 'blebs' is still not clear.

2. Definitions

We have previously reviewed those situations under which the ratios of amounts of cation transported to ATP hydrolyzed are substantionally less than the theoretical integer implied by the number of binding sites per monomer [28]. Some procedures cause irreversible uncoupling, whilst others are restored by return of the system to those conditions that favor coupling. The term uncoupling was first applied to oxidative phosphorylation by classical uncouplers such as dinitrophenol, which inhibit ATP synthesis and enhance flux of e^- through the respiratory chain of intact, but not of disrupted inner mitochondrial membranes. One of the key observations of Mitchell's chemiosmotic hypothesis was that mitochondria are able to accumulate and maintain a H^+ gradient, and that uncouplers dissipate this gradient. Dinitrophenol acts as an extramolecular protonophore, collapsing the gradient and inhibiting ATP synthesis. Intramolecular uncoupling refers to agents that dissociate proton flux from respiratory flux and of ATP synthesis and proton flux. An example of an intramolecular uncoupler is antimycin A.

Energy transducing systems, by definition, involve at least two processes, the driver and the driven. Unlike chemical reactions, there is no a priori reason to expect that coupling ratios should approach simple molar ratios. However, as the mechanistic processes of P-type ATPases became unraveled, it became clear that the number of binding sites per pump unit varied from one to three cations, and it was natural to expect that experimentally derived coupling ratios should be 2:1 for the Ca^{2+}-ATPase, and 3:2:1 for the Na^+/K^+-ATPase. Values for the gastric H^+/K^+-ATPase are less certain. A number of terms have been used to describe dissociation of energy transduction events, including variable stoichiometry, uncoupling, intramolecular and extramolecular uncoupling, and slippage. One of the aims of the present review has been to determine whether these terms may be used in a more specific sense.

2.1. Variable stoichiometry

Variable stoichiometry occurs when a P-type pump operates with less than the theoretical ratio of cations. For e.g. the Na^+/K^+-ATPase may turnover in the absence of Na^+, but maintains K^+ transport to give a 0:2:1 coupling stoichiometry. In the case of the Ca^{2+}-ATPase altering membrane lipids reduces the Ca^{2+} binding and transport stoichiometries from 2:1 to 1:1 [29].

2.2. Uncoupling

The term 'uncoupling' has been used to describe a variety of events and experimental conditions where the primary observation is that transport occurs at less than that expected for full coupling of scalar and vectorial transport.

2.2.1. Extramolecular uncoupling

Here the feature is that decreased coupling ratios are due to events extrinsic to the pump protein. Uncouplers of oxidative phosphorylation and ionophores are examples. The transport mechanisms are unaffected.

2.2.2. Intramolecular uncoupling

This is true uncoupling in the sense that the pump mechanism itself is altered. Uncoupling may be reversible or irreversible.

2.3. Reversible uncoupling

This is true uncoupling of the cation transport mechanism in that the catalytic cycle is so favored that one of the primary rules of coupling is violated [30]. This situation is perhaps the most useful avenue for exploration in that it gives clues as to the primary pump mechanisms.

2.4. Irreversible uncoupling

A number of reagents and procedures cause irreversible uncoupling. These include acid and thermal inactivation [31,32], covalent modification and site-directed mutagenesis (SDM) [33]. In general the process cannot be reversed by either chemical of physical means.

2.5. Slippage

We will suggest, based on the evidence reviewed here, that the term 'slippage' is reserved for those instances in which an intrinsic pathway of the ATPase is favored that leads to an uncoupled catalytic cycle, which is suppressed under physiological conditions. These are not new reaction paths, but ones which lead to violation of the transport 'laws'. An example is that of the Ca^{2+}-ATPase acting against a high transmembrane gradient [34]. Slippage will cause continuously variable coupling ratios from theoretical values down to zero. Slippage is a stochastic process, and depends on the probability of a coupled versus uncoupled pathways. The pump itself in unaffected and slippage is completely reversible.

2.6. Decoupling

This term has been applied to the process of mitochondrial oxidative phosphorylation, where reagents such as chloroform decrease ATP formation by decoupling H^+ transport due to a shunt, confined within the membrane itself, that is not in equilibrium with bulk medium [H^+] [35]. No example of this type of process has been described for the P-type cation pumps, but it is included here for completeness.

3. Structural features of the Ca^{2+}-ATPase relevant to slippage

Diverse methodologies, including electron microscopy [36], and other structural studies, concur as to the general shape of the Ca^{2+}-ATPase, and to its insertion into the lipid bilayer (for reviews see [37,38]). The overall architecture is that of a large cytoplasmic headpiece, stalk and transmembrane section. The phosphorylation site at Asp351 is located in the headpiece, together with the ATP binding site. Hydropathy plots identify 10 transmembrane helices, M1–M10 [39]. The headpiece splits on Ca^{2+} binding, suggesting that large conformational changes occur during turnover [40]. Ca^{2+} binding sites have been identified by SDM of intramembranous helices, involving M4–M6 and M8 [41].

Recently Toyoshima et al. [42] have succeeded in growing three-dimensional crystals of the Ca^{2+}-ATPase and have resolved its structure at 2.6 Å. This structure will be the foundation for the interpretation of many previous and future mechanistic studies. In general, it is remarkable how much the X-ray crystallographic data confirm previous more indirect studies, based on primary sequences, conserved residues, and mutagenesis, in the Ca^{2+}-ATPase, and how these complement those of similar data of the Na^+/K^+-ATPase and gastric H^+/K^+-ATPase. For the purposes of this review we will concentrate on those structural features of the Ca^{2+}-ATPase that have either direct or indirect bearing on slippage and uncoupling mechanisms.

The whole structure of the ATPase fits into a box of 100 Å × 80 Å × 140 Å [42]. This confirms previous models that place the catalytic domain 90 Å away

from the Ca^{2+} bindings sites [43]. A remarkable new feature arising out of the X-ray study is that some of the membrane helices, including M5, extend through the stalk region to the center of the cytoplasmic domain, P, thus identifying a structure that could transmit conformational signals from the catalytic active center to the intramembranous Ca^{2+} binding sites.

Previous models of the Ca^{2+}-ATPase predicted approximately equal lengths for the transmembrane helices. The X-ray data show that the lengths of the helices and their angles vary considerably. M2 and M5 are long ($\cong$60 Å), and relatively straight. M4 and M6 are partly unwound, and M10 is kinked in the center of the membrane. M2 and M3 are relatively long and isolated from other membranous helices. Extension of the membrane helices into the stalk corrects the previous suggestion that the stalk helices were separate entities from membrane helices [44].

3.1. Ca^{2+} binding sites

Previous studies by SDM suggested that the two Ca^{2+} binding sites are similar [33], and that they were stacked up inside a channel, with superficial and deep sites, I and II. However, ligands from M4, M5, M6 and M8, which constitute the two Ca^{2+} binding sites, as determined by the X-ray structure, show different folding patterns [42].

Crystals used to define the X-ray diffraction pattern were originally prepared in 10 mM Ca^{2+}. Two high density peaks were located in the intramembranous region, surrounded by M4, M5, M6 and M8. These were identified as Ca^{2+} on the basis (a) that their density is too high for water, (b) that at least six coordinating O atoms are located within 2.2–2.6 Å from the centers of each site, which is unusual for a water molecule, (c) that valency values, calculated from the geometry of the coordinating atoms, are 1.95 and 2.15 for sites I and II, confirming those predicted for Ca^{2+} binding sites [45], and (d) that a smaller peak 2.4 Å from Ca^{2+} (I) has a density like water.

The two Ca^{2+} sites are at similar heights with respect to the membrane and are 5.7 Å apart. They are termed sites I and II according to previous proposals, based on their affinities and access to surface medium [33]. Site I is located in a space between M5 and M6, with some contribution from M8 at 'a rather distal position' [42]. Side chain O atoms of Asn768 and Glu771 (M5), Thr799 and Asp800 (M6), and Glu908 (M8) contribute to this site, confirming mutational studies [41]. All of the side chain O atoms are arranged in the same plane relative to the membrane, except for Glu771, which coordinates from the lumenal side. Disruption of helix geometry of M6 around Asp800 and Gly801 allows both Thr799 and Asp800 to contribute ligands for binding of Ca^{2+}.

Site II has a different coordination to site I. It is formed almost 'on' helix M4 by main chain carbonyl O atoms of Val304, Ala305, and Ile307 of M4, and side chain O atoms of Asn796, Asp800 (M6) and Glu309 (M4). Coordination to main chain carbonyls is possible due to unwinding of helix M4 between Ile307 and Gly310. The motif PEGL appears to be a key sequence in P-type ATPases. The glutamate residue is replaced in heavy metal pumps by either cysteine or histidine [46].

Ca^{2+} binding sites appear to be stabilized by H-bonded networks between coordinating residues, e.g. Val306 on Asn768, and between residues on different helices, e.g. Val304 and Glu309 on M4 and Glu58 on M1. Toyoshima et al. [42] have proposed that H-bonded networks are important for cooperative binding of the two Ca^{2+} ions [47]. Correct positioning of Asp800 appears to be important for function. It is located in the unwound portion between the two helices that constitute M6, and its carbonyl O is highly exposed.

3.2. Pathway for Ca^{2+}

The Ca^{2+}-ATPase does not have a large vestibule, as is seen in ion channels [48]. One possible space is the area surrounded by M2, M4 and M6, which is a wide open cavity that appears to be water accessible since it contains seven H_2O molecules. In the upper part of this cavity are Gln108 and Asn111, a critical residue for ATPase activity. Rows of exposed O atoms are formed by the unwound part of M4 (Pro312 to Glu309), and of M6 (Asp800 and Gly801). The rows of main chain carbonyls that line this cavity may provide a pathway to the Ca^{2+} sites, since they constrict near the Ca^{2+} binding sites, trapping a H_2O molecule. A critical feature here is

that the O atoms are arranged in nearly ideal geometry to bind H_2O that is bound more tightly than to monovalent or divalent cations. The exit from the Ca^{2+} sites might be located in the area surrounded by M3–M5. A ring of O atoms with bound water molecules is also provided here. Unwinding of transmembrane helices appears to be a key event in providing ligands for Ca^{2+} binding. Firstly it provides the coordination geometry of Ca^{2+} ions, and secondly exposes rows of O atoms that both guide Ca^{2+} to its binding site, and at the same time removes hydration shell water from the cation.

The characteristics of binding of Ca^{2+}, with independent and coexisting high affinity sites, suggest a channel-like transmembrane structure. Release of two $^{45}Ca^{2+}$ ions is sequential [49]. Both ions are displaced by EGTA (ethylene bis(oxyethylene nitrilo) tetraacetic acid), but only one is flushed out with $^{40}Ca^{2+}$. This suggests that binding is a two step reaction, where the superficial ion appears to lock in the deeper site. Low affinity binding to E_2 sites is also sequential and ordered [50]. However, after binding to E_1 with a prebuilt order of $^{45}Ca^{2+}$ and $^{40}Ca^{2+}$, the sequential property is lost [51]. The process that alternates Ca^{2+} from cytoplasmic to lumenal sites appears to result in scrambling, possibly in the intermediate occluded state [52].

The channel model, which implies multiple in-line sites, is not supported by the X-ray crystallographic model. Crystals were originally prepared in 10 mM $CaCl_2$ that favors the E_2 conformation. Further structural studies on alternate conformations may explain the discrepancies, since kinetic data have suggested four or possibly six Ca^{2+} binding sites [52].

4. Occluded cations in P-type ATPases

The properties of cation binding sites of the P-type ATPases have been well established, particularly with respect to the Ca^{2+}-ATPase and Na^+/K^+-ATPase. In general two major conformations have been established with respect to their cation site accessibility and binding affinities. Using the conventional nomenclature, cytosolic-orientated sites have high affinities for the primary transported cation, i.e. Ca^{2+}, Na^+ and H^+. These alternate with low affinity sites that are orientated to either the lumen of SR or towards the extracellular fluid. According to the alternating access model, energy barriers that act as a gating system block exchange at these sites and are required to prevent back diffusion down the energy gradient.

In addition to sites that have alternating access, a third category, the occluded state, does not have access to either membrane surface (for review see [6]). Maximum amounts of the occluded species occur when E_1-P is the predominant intermediate. Under physiological conditions occluded forms are transient. However under conditions that maximize E_1-P, e.g. acceleration of formation, and inhibition of E_1-P decay, occluded cation intermediates are stable enough to be isolated by gel column filtration.

4.1. Occluded species on the Ca^{2+}-ATPase

Sepersu et al. [53] showed that CrATP traps two Ca^{2+} ions on the Ca^{2+}-ATPase, and the complex is stable for several hours. CrATP binds with Ca^{2+} to the ATPase, which is then solubilized in $C_{12}E_8$, and has led to the conclusion that the monomeric species is capable of Ca^{2+} occlusion [54]. Varying proportions of E_1-P/E_2-P parallel the ability of the enzyme to occlude Ca^{2+}. The stoichiometry of occluded Ca^{2+} sites is two per phosphorylation site [55–60] in the form of E_1-P$\langle 2Ca^{2+}\rangle$ [61]. There is general agreement that decreased affinity and altered accessibility of the low affinity binding sites precede hydrolysis of E_2-P.

4.1.1. Occluded Ca^{2+} in the Ca^{2+}-limited state

We have recently characterized a steady state of the Ca^{2+}-ATPase in vitro that is analogous to the relaxed state in skeletal muscle [62]. SR vesicles are incubated in the presence of limiting amounts of Ca^{2+} (<10 μM total), ATP and oxalate. Medium $[Ca^{2+}]_{free}$ decreases rapidly to a limiting value $[Ca^{2+}]_{lim}$ of approximately 50 nM, and transport stops. Oxalate clamps intravesicular Ca^{2+} to less than 10 μM, giving $[Ca^{2+}]_{in}/[Ca^{2+}]_{out}$ of 200:1. This is less than a dynamic equilibrium of 10 000:1, based on the hydrolysis of ATP of 56 kJ/mol.

Under these conditions addition of thapsigargin (TG), a specific inhibitor of the Ca^{2+}-ATPase, re-

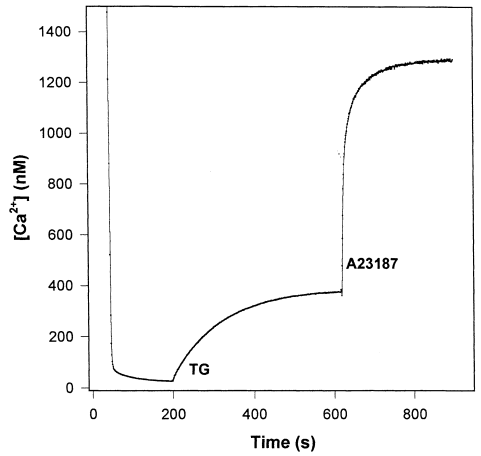

Fig. 3. TG-induced Ca^{2+} release from the Ca^{2+}-ATPase in the Ca^{2+}-limited state (Berman, [52]).

leases 1–2 mol Ca^{2+}/mol Ca^{2+}-ATPase [52] (Fig. 3). TG binds with high affinity and specificity to all intermediates of the Ca^{2+}-ATPase. However, it is competitive with Ca^{2+} because it promotes the irreversible reaction, $E_2{\cdot}TG \rightarrow E_2^A{\cdot}TG$, a stable form of E_2 that cannot be phosphorylated by P_i [63]. TG thus causes release of Ca^{2+} since it depletes the catalytic cycle of intermediates. Maximum release of Ca^{2+} by TG occurred within 20 s of addition of ATP to initiate transport, and was 3.0 nmol/mg or 0.75 mol/mol Ca^{2+}-ATPase. It declined with time with a decay constant of 0.13 min^{-1} and was 0.4 nmol/mg after 1000 s.

Simulations indicate that total Ca^{2+}, bound to all intermediates of the catalytic cycle, is less than 1% of total catalytic intermediates. Release of Ca^{2+} from intravesicular stores can be excluded since ionophore A23187 (calcimycin), or Triton detergent, releases Ca^{2+} that has been actively transported. Release was independent of ADP and was also observed with acetylphosphate (AcP) as substrate, excluding reversal of catalysis. These findings lead to the conclusion that occluded Ca^{2+}, presumably as E_1-P.[2Ca], exists independently of high and low affinity sites. Coexistence of the three classes can be explained on the basis of a channel-like structure. The fact that occluded Ca^{2+} can be detected whilst the Ca^{2+}-ATPase is in the Ca^{2+}-limited state needs to be considered in possible models, and has implications which favor a channel-like mechanism of ion transport.

4.2. Occluded sites on the Na^+/K^+-ATPase

Indirect evidence for the existence of occluded species was first obtained from the red blood cell sodium pump [64]. Na^+–Na^+ exchange requires both ATP and ADP and is blocked by oligomycin, which also inhibits the conversion of E_1-P to E_2-P. Glynn et al. reported that under conditions of low ADP, and in the presence of *n*-methylmaleimide (NEM) that favors the formation of E_1-P, three Na^+ are occluded [65,66]. Vilsen et al. [67], using CrATP, characterized a state, $E_1{*}P{\cdot}3Na^+$, that is stable for hours and can be solubilized and retained following column chromatography. Occluded Na^+ must dissociate during the E_1-P to E_2-P isomerization [68] since E_2-P does not contain the occluded species.

Post et al. [69] first described evidence for an occluded K^+ (Rb^+) species. The kinetic behavior of unphosphorylated E depended on the K^+ cogener. They suggested that an occluded K^+ species existed as $E_2\langle K^+\rangle$ and was released after the slow isomerization step to E_1. This step is also accelerated by ATP [6,67,70]. Glynn [71,72] showed that the Na^+/K^+-ATPase can retain $^{86}Rb^+$ when passed down a cation exchange column, and stoichiometry of the site is two K^+ per E-P [71–74]. ATP and Na^+ prevent occlusion by favoring E_1. There are therefore two routes for K^+ occlusion [6]. Under physiological conditions that favor the forward reaction, K^+ becomes occluded after hydrolysis of E_2-P. In the reverse reaction K^+ binds to E_1, undergoes a conformational change to E_2, and becomes occluded.

4.3. Ordered release of K^+ from the Na^+/K^+-ATPase

Ordered release of K^+/Rb^+ by the Na^+/K^+-ATPase to the intracellular surface explains the kinetics of $^{86}Rb^+$ release and its inhibition by cations with $Tl^+ > Rb^+ > K^+ > Cs^+$ [75–78]. This is analogous to that observed for ordered binding and release of Ca^{2+} from the Ca^{2+}-ATPase. In order to explain the kinetics of blocking of $^{86}Rb^+$ release by cogeners, Forbush [75] has suggested that release of K^+ from the channel is limited by inhibition at its neck ('leaky pocket'), or by intermittent opening of the channel ('flickering gate'). The latter mechanism is favored since the rate constant, k, for E_1-$^{86}Rb^+ \rightarrow E_2$-$^{86}Rb^+$ is independent of Rb^+ concentration.

5. Uncoupling of energy transduction in P-type cation pumps

A wide variety of reagents and procedures lead to dissociation of vectorial and scalar activities of P-type pumps. By far the majority of studies have been carried out on the Ca^{2+}-ATPase and Na^+/K^+-ATPase, presumably for the reason that the catalytic cycles and transport activities have been best defined in these systems. Uncoupling of the SR Ca^{2+}-ATPase has been the subject of a previous review in 1982 [28]. Since that time many further instances of uncoupling or slippage have been reported in P-type cation pumps, and previous postulates have been confirmed.

5.1. Irreversible uncoupling of the Ca^{2+}-ATPase of SR

5.1.1. Ageing

Like Ebashi and Lippman [79], who noted uncoupling of SR vesicles at 4°C, Keilie and Myerhoff [80] described similar effects, but were unaware that their 'Mg^{2+}-ATPase' was in fact Ca^{2+}-dependent, since they did not have access to specific Ca^{2+} chelators such as EGTA. In general Ca^{2+} transport activity is more sensitive to physical extremes than ATP hydrolysis.

5.1.2. Thermal denaturation and occluded cations

Relatively mild procedures uncouple Ca^{2+} transport activity from Ca^{2+}-dependent ATPase activity of SR. Incubation at 37°C for 5 min at pH 5.6 leads to more than 90% inhibition of transport, whilst ATPase activity increases [31]. Some increase in permeability to Ca^{2+} was also noted, but seemed to be insufficient in view of the extensive uncoupling. Transport activity was protected by millimolar Ca^{2+}, Sr^{2+} and Mn^{2+}, but not by Ba^{2+} or La^{3+}. The protective Ca^{2+} binding sites are identical to the Ca^{2+} transport sites and those that activate ATP hydrolysis. Thermal denaturation also occurs at pH 7.0 and 37°C in the presence of EGTA [32]. Ca^{2+} protective sites are in the micromolar range with $n_{H(Ca)} = 2$, suggesting that this is an intramolecular uncoupling process involving the pump protein. Temperature dependence of EGTA uncoupling occurred with E_a of 271 kJ/mol [32], which was increased to 353 kJ/mol with saturation of high affinity Ca^{2+} sites. High activation energies are compatible with partial unfolding of the Ca^{2+}-ATPase.

Lepock et al. [81] have studied thermally induced uncoupling with EGTA at 37°C of isolated SR vesicles by means of differential scanning calorimetry. They have confirmed that the uncoupling is intramolecular with no major increase in membrane permeability. Thermal analysis showed at least two unfolding events at 30 and 40°C. No heat capacitative events were correlated with uncoupling of transport. They have concluded that unfolding of the catalytic cytoplasmic domain was consistent with the 30°C site, whilst unfolding the intramembranous domain gave rise to the more heat resistant process. There is some uncertainty regarding this interpretation since contamination by phosphorylase in the SR vesicle preparations could be responsible for the second unfolding event. However it is clear that intramolecular uncoupling of the Ca^{2+}-ATPase is due to only a partial unfolding of the protein. Thermal denaturation of the Ca^{2+}-ATPase thus reveals two thermodynamically independent domains. In further studies it has been shown [82] that uncoupling by EGTA is due to a thermotropic conformational change in the Ca^{2+} binding domain of the ATPase. Dibucaine, which sensitizes the coupling mechanism to thermal inactivation of transport [83], has no effect on ATP hydrolysis.

Thermal uncoupling can be reversed by solubilization in detergent and reconstitution into the original physiological lipid vesicles [84]. Transport recovered is 50% of the original coupled activity, which signifies total reversal of uncoupling, allowing for random insertion of Ca^{2+}-ATPase into reconstituted vesicles. This finding also confirms that there is no covalent modification, such as thiol oxidation, in the uncoupled state. Interaction of the Ca^{2+}-ATPase with membrane lipids appears to constrain the Ca^{2+}-ATPase in the uncoupled conformation.

SR vesicles, incubated with millimolar Ca^{2+}, in the absence of ATP, form a stable 'tightly bound' Ca^{2+} species that is not removed by extensive washes [85]. This species does not have free access to both sides of the membrane and may represent the physiological occluded species that is formed by E_1-P.Ca_2. The ability of the Ca^{2+}-ATPase to become enriched with tightly bound or 'occluded' Ca^{2+} has been correlated

with coupled energy transduction, since incubation in EGTA at 37°C causes simultaneous loss of transport activity, and of tightly bound Ca^{2+}.

Partial denaturation that results in uncoupling leads to several predictions with respect to structure and function of P-type cation pumps. Firstly, since the pump unit is a single polypeptide species, it is an indication that scalar and vectorial events must be spatially separate. A question arises as to whether the uncoupled state is an intermediate along the pathway to complete unfolding of the Ca^{2+}-ATPase. The molten globule state (MGS) has been implicated in both folding and unfolding [86]. It is generally assumed that the MGS is a global intermediate and that all domains of the protein are equally unfolded and expose hydrophobic interior sites to the medium. There is however a precedent in the case of independent unfolding of the domains of diphtheria toxin [87], in which one region is denatured, whilst the other remains in the native state.

The ATP analogue, 2′(3′)-*O*-(2,4,6-trinitrophenyl) (TNP)-ATP, binds to the nucleotide binding site of the Ca^{2+}-ATPase with higher affinity than for ATP and with increased fluorescence. Turnover of the enzyme results in a unique phenomenon, characteristic of the Ca^{2+}-ATPase, i.e. a several fold fluorescence increase or 'superfluorescence' [88]. This has been shown to be due to increased hydrophobicity at the active site in the E_2-P state. Reverse phosphorylation from P_i, in the presence of EGTA, also results in superfluorescence. Superfluorescence from both reactions is decreased in EGTA-uncoupled SR [89]. This means that the species E_1-P.2Ca^{2+}, which has a relatively hydrophilic substrate binding site, predominates during uncoupled turnover, and that its hydrolysis via an alternate uncoupled pathway, with release of Ca^{2+} to the cytoplasmic membrane surface, is favored. The result is a violation of one of the rules of coupling, described by Jencks [90].

A working hypothesis might therefore be that the uncoupled state is a partially unfolded restricted domain within the Ca^{2+}-ATPase that simultaneously exposes the catalytic site to the medium, and prevents isomerization to E_2-P, which is known to have a relatively hydrophobic ATP binding site. There is also failure to transmit conformational changes at the catalytic site via membrane helices that extend into the stalk region.

Tryptic digestion of pig kidney Na^+/K^+-ATPase in the presence of Na^+ or K^+ leads to the loss of the bulky cytoplasmic catalytic domain and retention of a characteristic 19 kDa intramembranous C-terminal peptide [91]. A remarkable property of the preparation is the ability to occlude $^{86}Rb^+$ in the absence of phosphorylation by ATP. Further digestion with non-specific proteases in the absence of monovalent cations and the presence of Ca^{2+} confirmed that the 19 kDa peptide is responsible for the occluded site [92]. Of special interest here is the fact that incubation of 19 kDa membranes in the absence of monovalent cations leads to rapid loss of the ability of the preparation to occlude $^{86}Rb^+$ [93]. Cations Na^+, K^+ and Rb^+ protect against deocclusion, but sodium antagonists, *p*- or *m*-xylyleneguanidium, guanidinium ions and ethylenediamine were ineffective.

Kinetics of thermal inactivation have been fitted to the data in the range 25–30°C to a two step model, interconverting native species, N, reversibly unfolded intermediate, U, and irreversibly denatured, I [94]. Correlation of loss of occlusion with loss of fragments of the 19 kDa membrane indicates that interactions between M5/M6 and M7/M10 appear to be essential for Rb^+ occlusion.

It appears, therefore, that both in the case of the Ca^{2+}-ATPase and Na^+/K^+-ATPase, the occluded state is formed under specific conditions. Thermal inactivation at 37°C, in the absence of the transported cation (Ca^{2+}, Na^+ or K^+), leads both to the loss of the occlusion site, and, at least in the case of the Ca^{2+}-ATPase, to the uncoupled state. Perhaps thermal inactivation and uncoupling are due to a minor localized irreversible unfolding of critical sites on the ATPases that convert bound cations to the occluded forms.

Several lines of evidence indicate that the degree of coupling of transport depends critically on the fate of Ca^{2+} bound to E_1-P. At this branch point the catalytic cycle can either proceed in the coupled mode by isomerization to E_2-P.2Ca, or be diverted to an uncoupled hydrolysis path, $E_1\text{-P.2Ca} \rightarrow P_i + 2Ca^{2+}_{out}$, with release of Ca^{2+} to the external cytosolic membrane surface.

There are several examples of diversion of intermediate fluxes during turnover of the Ca^{2+}-ATPase, where an uncoupled pathway is favored. Kawakita et al. [95] have described how covalent modification of

the ATPase with NEM slows turnover and favors an uncoupled pathway. This may be explained by the finding [96] that NEM inhibits the isomerization step E_1-P.2Ca ↔ E_2-P.2Ca, favouring accumulation of the E_1-P species and diversion of flux of intermediates towards the uncoupled pathway.

Native and reconstituted SR vesicles show variable stoichiometry when lumenal Ca^{2+} rises [97]. This phenomenon has been explained by a branched pathway with hydrolysis of E_1-P before release of Ca^{2+} into the lumen. The reaction sequence, described by MacLennan et al. [33], includes a reaction bypassing E_2-P, linking E_1-P.2Ca and unliganded E_1 or E_2 directly. McIntosh and colleagues [98,99] have described a unique effect of glutaraldehyde on the 110 kDa Ca^{2+}-ATPase. The cross-linked enzyme is readily identified by its anomalous electrophoretic behaviour, where it migrates like a 125 kDa species. Glutaraldehyde causes an intramolecular cross link of Lys492 and Arg678 at the active site. The three reactions, Ca^{2+} binding, Ca^{2+} occlusion, and release of Ca^{2+} to the lumen, are blocked by glutaraldehyde, leading to the suggestion that two sequential hinge bending movements lead to closure of the site in the native enzyme. Cross linking blocks the formation of E_2-P, with the result that Ca^{2+} is released from E_1-P.2Ca to the cytoplasmic surface when E_1-P is hydrolyzed directly.

The ATP analogue $8N_3$TNP-ATP, unlike TNP-ATP, undergoes slow Ca^{2+}-dependent hydrolysis [100]. Photoactivation causes the nucleotide to be covalently bound to Lys492. The tethered nucleotide/enzyme complex can still undergo hydrolysis, which is, however, uncoupled from Ca^{2+} transport. Unlike the glutaraldehyde-modified enzyme, in which the E_1-P to E_2-P is inhibited, with low superfluorescence of TNP-ATP, photoinactivation leads to uncoupling of Ca^{2+} transport with no change in superfluorescence. It has been postulated that coupling involves relocation of Lys492, and catalysis requires separation of Lys492 and Arg678 [100].

5.1.3. Uncoupling procedures and efflux

A number of chemical procedures, and low and high pH treatment, uncouple transport of Ca^{2+} [28,101,102]. Another group of uncoupling reagents, including hydrophobic drugs [103,104], arsenate [105] and heparin [106], uncouple by promoting efflux through the Ca^{2+}-ATPase. The question arises as to what these procedures have in common. All bind to E_2 in competition with P_i, and promote uncoupling when intravesicular Ca^{2+} rises and effluxes via the Ca^{2+}-ATPase pump protein. Reversal of the cycle, in the presence of P_i and dimethylsulfoxide (DMSO), promotes phosphorylation of E_2 in the steady state [34,107,108].

5.2. Uncoupling of yeast and plant plasma membrane P-type H^+-ATPases

Plasma membrane P-type ATPases from yeast and plants transport H^+ outwards and function both to promote solute uptake by secondary transporters, and to regulate cytoplasmic pH. The yeast enzyme catalyzes ATP and AcP hydrolysis [109]. Both form similar E-Ps and protect against tryptic digestion, indicating that they promote similar conformational states. However, AcP is unable to drive proton transport. A S368F mutant enzyme is insensitive to vanadate inhibition with ATP but becomes sensitive with AcP. It has been concluded that with AcP there is a branched pathway, or short circuit, that bypasses E_1-P, since vanadate inhibits the E_2 state. The mutant Ile183 in S2 to alanine partially uncouples H^+ transport [110,111]. Multisite mutants in both S4 and S5 by helix-breaking proline indicate that the native state has been optimized for length and interactions with other stalk elements [112].

Yeast cells, when incubated with glucose after starvation, show a 50-fold increase in H^+ extrusion and only 8-fold increase in ATPase activity, indicating that the H^+-ATPase is uncoupled in the starved state [113]. This intrinsic uncoupling is the physiological response for regulation of pump activity.

Mutants of the plant *Arabidopsis thaliana* H^+-ATPase (AHA1) have been cloned and isolated from yeast cells [114]. A Trp874Phe substitution produced a modified enzyme with 2–5-fold increase in ATPase activity, without any extrusion of H^+ from transformed yeast cells. It has been concluded that Trp874 is involved in controlling the degree of uncoupling of plant AHA1. Similarly, a mutant Asp684Asn of AHA2, located on M6, has been expressed, which is conserved in all P-type ATPases, and which coordinates Ca^{2+} in the sarco- and endoplasmic reticulum Ca^{2+}-ATPase 1 (SERCA1). The

mutant hydrolyzes ATP but does not pump H^+ [115]. The mutant enzyme was insensitive to vanadate, which binds to E_2, and the intermediate E-P species was sensitive to ADP. On this basis it was concluded that the mutant was locked in the E_1 conformation, and unable to undergo the E_1-P ↔ E_2-P transition.

6. SDM and uncoupling

SDM has played a major role in elucidating functions of domains and individual amino acids of the Ca^{2+}-ATPase, including E_1-P, E_2-P, phosphorylation-negative, ATP affinity, Ca^{2+} affinity and TG binding site mutants. Activities in the microsomal fraction of mammalian COS-1 cells have been analyzed for Ca^{2+}-ATPase activity, E-P levels, and $^{45}Ca^{2+}$ uptake [116]. Preparations contain little endogenous activities. Sorensen and Andersen [117] have prepared mutants of residues at the boundary of transmembrane segment M5 and the connecting stalk region S5 and have shown that some of these play a central role in energy coupling.

Mutagenesis of key amino acids may be expected to cause intramolecular uncoupling, as previously defined [28], with no or little increase in efflux, either through the intact lipid bilayer or via the Ca^{2+}-ATPase (for review see [118]). Mutant Tyr763 → Gly, located at the membrane boundary, connecting M5 to the catalytic site, has interesting properties [119]. The mutant catalyzes ATP hydrolysis but does not transport $^{45}Ca^{2+}$. Ca^{2+}-ATPase turnover appears to proceed via both ADP-sensitive and -insensitive E-P, depending on pH, K^+ and Mg^{2+}. The uncoupled mutant appears also to be able to occlude Ca^{2+} in the presence of CrATP, which stabilizes the native form for hours. Uncoupling is thus a defect in a step during the latter part of the catalytic cycle. It has been suggested that the mechanism of uncoupling is due to a problem with gating by the bulky side chain of the Ca^{2+} binding sites, after the lumenal gate is opened in E_2-P and E_2 forms [116].

Another mutant Lys758 → Ile has similar properties to Tyr763 → Gly. Addition of ionophore A23187 to Tyr763 → Gly does not enhance turnover due to its inability to form a Ca^{2+} concentration gradient. Unlike Tyr763 → Gly, Lys758 → Ile accumulates Ca^{2+} in the presence of oxalate, which can be explained by the step E_1-P → E_2-P no longer being sensitive to high intralumenal Ca^{2+}. There is also the possibility that leakage through the mutant Ca^{2+}-ATPase, in the E_2 form, is similar to efflux, as is seen with other uncoupling agents [103–105]. A feature of the Lys758 → Ile mutant is that it dephosphorylates rapidly at pH 8.4, whilst dephosphorylation of the wild type is inhibited. It has been suggested [117] that a salt bridge is formed in native ATPase between Lys758 and a negatively charged side chain.

7. Slippage on the Ca^{2+} pump of SR

Under ideal conditions for coupled transport, Ca/ATP ratios approach theoretical maximum. Conditions expected to alter the relative concentrations of catalytic cycle intermediates can decrease the ratio over a wide range.

7.1. Slippage at high lumenal [Ca^{2+}]

Isolated SR vesicles have provided a near ideal system for measurements of Ca^{2+} transport. As derived from white fast twitch muscle (e.g. hind and back leg muscle from rabbits) they form discrete vesicles, with an internal volume of approximately 4–5 μl per mg of Ca^{2+}-ATPase [85]. In addition they are well sealed and orientated such that the majority of the pump units face the outside, equivalent to the cytoplasmic surface, and are well sealed. The SR vesicles from muscle preparations may be separated into terminal (junctional or heavy) vesicles, which contain most of the ryanodine receptor, through which rapid efflux of Ca^{2+} causes contraction, and the light, or cisternal SR, which contains the Ca^{2+} pump units, and are free of efflux channels. For these reasons isolated intact SR light vesicles have been well characterized, and are suited for the study of energy transduction, and the coupling of scalar events of the catalytic cycle with vectorial steps that lead to active transport.

Early experiments showed a 2:1 ratio of Ca^{2+} transported to that of ATP hydrolyzed [120] with the use of oxalate to extend the time of measurement. This finding was in keeping with cooperative binding of two Ca^{2+} ions for activation of catalysis

[47,120]. Ratios of Ca^{2+}/ATP of 2.0 are only observed when $[Ca^{2+}]_{in}$ is low due to complexation with oxalate resulting in a pseudo-steady state [121], or in the presteady state before $[Ca^{2+}]_{in}$ rises to inhibitory free levels of approximately 1 mM [122]. Coupling ratios of less that 2.0 under a variety of experimental conditions have generally been explained by leakage of Ca^{2+} through pathways other than that of the Ca^{2+}-ATPase. Free lumenal Ca^{2+} in the presence of oxalate is maintained below 10 μM [120]. Uptake of Ca^{2+} and rates of hydrolysis remain constant, and Ca^{2+}/ATP ratios are maintained at $\cong 1.5$ for several minutes, while intralumenal Ca^{2+} is below the $K_{0.5}$ of low affinity Ca^{2+} sites causing back inhibition. In the absence of oxalate, and at 10°C, the Ca^{2+}/ATP ratio is decreased within a few seconds [97]. TG, which blocks Ca^{2+} transport and ATPase, does not result in Ca^{2+} efflux from Ca^{2+}-loaded vesicles, which excludes a significant leakage of Ca^{2+} under the conditions of the assay. However, medium and lumenal Ca^{2+} undergo rapid exchange that is blocked by TG. The absence of ADP ↔ ATP or P_i ↔ ATP exchanges at maximal uptake levels is due to low levels of ADP and P_i. These experiments, performed in the presence and absence of oxalate, suggest that high lumenal Ca^{2+} favours hydrolytic cleavage of E_1-P.2Ca through an alternate pathway that results in P_i release with no net uptake of Ca^{2+} into the lumen of vesicles [3,97,123].

Lipid bilayers are highly impermeable to Ca^{2+}. Minimal contribution by the Ca^{2+} physiological release channel can be obviated by use of pure preparations of Ca^{2+}-ATPase from 'light' vesicles. Passive leakage has been ascribed to either the Ca^{2+}-ATPase itself [34,101,103,124,125], or through an as yet unidentified protein. A feature of this leakage is that it is blocked by micromolar medium Ca^{2+} [34]. Calcium uptake by reconstituted vesicles, containing purified Ca^{2+}-ATPase, is also inhibited by lumenal Ca^{2+} [101,124,125]. Sub-stoichiometric values of coupling ratios have been attributed to leakage of Ca^{2+} through unspecified routes or channels. Passive leakage through the Ca^{2+}-ATPase, uncoupled from ATP synthesis, is one manifestation of slippage of the Ca^{2+} pump, and has been demonstrated in reconstituted vesicles [34,97]. In addition, spontaneous Ca^{2+} release when turnover occurs, either due to removal of substrate or by inhibitors of the pump, is not due to pump reversal since it is also seen with AcP as substrate, where the absence of ADP makes reversal impossible [126,127].

Reconstituted vesicles, which have relatively low amounts of Ca^{2+}-ATPase relative to intravesicular volume, can take up Ca^{2+} in a linear fashion for longer periods than for native SR, but eventually do decrease Ca^{2+} uptake, whilst ATPase activity is unimpaired [97], which has been attributed to slippage of the pump.

Yu and Inesi [97] and Inesi and de Meis [34] have characterized the factors that limit steady state filling of sealed SR vesicles by active transport. Under these conditions uptake is enhanced by 1 mM P_i, which although below the saturation level for $Ca_3(PO_4)_2$ precipitation, nevertheless by forming a complex removes the driving force for the back reaction. Uptake of Ca^{2+} is further favored by scavenging ADP with an ATP regenerating system, and by the solvent DMSO. Steady state conditions were $Ca_3(PO_4)_2$ complex $\cong 10$ mM, and free $[Ca^{2+}]_{in}$ in lumen of 0.33 mM. DMSO (20% v/v) enhanced uptake [34], which could be explained by a more favorable complexation of Ca^{2+} and P_i, by regulation of the catalytic cycle, or by reducing the affinity of E-P for ADP. The DMSO effect is only seen under conditions of low pump efficiency. With AcP as substrate, uptake is high and there is no enhancement by DMSO, which may in fact cause some inhibition. With ADP there is enhanced ATP ↔ P_i exchange [34,128]. In the presence of DMSO there is increased efficiency (Ca^{2+}/ATP ratio) of the pump due to higher reverse activity and lower transport rate [34]. Nevertheless, with increased filling of vesicles with Ca^{2+}, net uptake diminishes after approximately 40 min, with a pump efficiency of approximately 0.1 and only limited inhibition of Ca^{2+}-ATPase activity.

7.2. Ca^{2+} leakage via the Ca^{2+}-ATPase

High conductance channels (ryanodine receptor) [129,130] are absent in vesicles prepared from 'light' cisternal SR. The measured low leakage rate of 0.4 min^{-1} which is inhibited by micromolar Ca^{2+} is readily distinguished from the high conductance pathway, $k = 10\ s^{-1}$, which is activated by Ca^{2+} [131]. Purified reconstituted vesicles have a similar low conductance [125,132,133]. Even though leakage

is slow under passive conditions, Inesi and de Meis [34] have suggested that the same pathway is rendered more permeable under conditions of pump turnover, allowing a more effective leakage when high lumenal Ca^{2+} and ADP are present. This represents slippage of the pump rather than leakage through independent pathways.

Inesi and de Meis have proposed a reaction scheme, modified to include slippage [34], that is based on the original cycle of de Meis and Vianna [5]. It includes additional steps for Ca^{2+} binding and dissociation [47,134], kinetic effects of ADP [135] and ATP modulations of some intermediate reactions [136,137]. The interdependent effects of high lumenal Ca^{2+} and ADP are explained by a prominent shift to ADP-sensitive E_1-P.Ca_2 [138]. This results in a high rate of ATP $\leftrightarrow$ P_i exchange without net Ca^{2+} uptake. It is suggested [34] that Ca^{2+} slippage through the Ca^{2+}-ATPase channel into the external medium occurs under turnover conditions, when high ADP and lumenal Ca^{2+} are present. Under these conditions hydrolysis of E-P occurs with lower coupling ratios. Rossi et al. have made similar suggestions to explain the low transport stoichiometries measured with alternate substrates [139].

Concentrations of myoplasmic P_i in the millimolar range are expected to complex with lumenal Ca^{2+}. Levels of [ADP] in vivo are in the range 1×10^{-6}–1×10^{-5} M due to regeneration systems and binding to myoplasmic proteins [140], and may well be within the range that would control E_1-P.$2Ca^{2+}$ levels.

The reconstituted proteoliposome system, described by Levy et al. [141], has several useful experimental properties. The liposomes are large (100–200 nm) with four to five pump units per vesicle, and the lipid environment of the Ca^{2+}-ATPase can be readily manipulated. Since Ca^{2+}-ATPase units are randomly inserted into the membrane, this results in a measured activity of 50% of that of purified ATPase. A significant feature of this system is that during active transport lumenal Ca^{2+} rises slowly so that Ca^{2+}/ATP ratios can be readily measured over prolonged periods. Like native SR vesicles, residual ATPase activity persists when liposomes are filled and transport ceases. This activity is inhibited by EGTA, so that it is still dependent on medium Ca^{2+}. Inhibition of reconstituted Ca^{2+}-ATPase with TG blocks both uptake and release, so that these vesicles have no measurable Ca^{2+} leak. These studies show that in both native SR vesicles and in reconstituted proteoliposomes the decreased coupling ratios from the maximum of 2.0 on vesicle filling are not due to passive leakage of Ca^{2+}, but are an intrinsic feature of the Ca^{2+}-ATPase pump unit.

SR vesicles support active transport of Sr^{2+}. Initially it was reported that Sr^{2+}/ATP ratios were 1.0, in agreement with the proposal that this cogener binds to a single site per Ca^{2+}-ATPase monomer [142,143]. However, Sr^{2+}/ATP ratios measured by a continuous stat method were similar to those of Ca^{2+}/ATP [144–147], but with lower affinity for the Ca^{2+}-ATPase before and after phosphorylation. Compared to those for Ca^{2+}, maximum levels of Sr^{2+} uptake are greater, due to a higher $[Sr^{2+}]_{in}$ that is required to saturate inward orientated sites [148]. There is no significant leakage of Sr^{2+} after TG inhibition (unpublished observation).

Flux through an alternate pathway before release of bound Ca^{2+} or Sr^{2+} could explain the decrease in coupling ratio with increasing $[M^{2+}]_{in}$. The fact that $Ca^{2+}_{in} \leftrightarrow Ca^{2+}_{out}$ exchange occurs in the absence of ATP $\leftrightarrow$ ADP and $P_i \leftrightarrow$ ATP exchanges indicates that alternate pathway flux is significant [97]. The ratio of Ca^{2+}/ATP declines to 0.11 when $[Ca^{2+}]_{in}$ = 10 mM. It is also affected by the affinity of E_2-P for lumenal Ca^{2+}, and explains why Sr^{2+}, which has lower affinity for E-P than for Ca^{2+}, gives higher Sr^{2+}/ATP coupling ratios.

There is considerable evidence that the only significant leakage of Ca^{2+} is through the Ca^{2+}-ATPase [34,101,125,127,149]. Leakage is inhibited by external Ca^{2+} binding to sites having identical affinity and positive cooperativity to that of the high affinity sites on E_1 [34]. A similar leak occurs from vesicles reconstituted from purified ATPase and phospholipids [101,125,149]. Leaks occur in vesicles lacking ryanodine receptor [34]. Variable stoichiometry also occurs when larger reconstituted vesicles are filled. Several studies have confirmed that reconstituted vesicles have low ionic permeability [34,141,150–152].

7.3. *Effects of membrane phospholipids on slippage of the Ca^{2+}-ATPase*

Dalton et al. [153] have studied the effects of lipid composition in reconstituted vesicles on ATPase ac-

tivity, Ca^{2+} transport and slippage, using a modification of the method of Rigaud et al. [154]. These are relatively large vesicles (120 ± 30 nm), with a trapped volume of 174 μl/mg. The concentration of outward orientated ATP sites was 0.03 μM. Carbonylcyanide *p*-trifluoromethoxyphenyl hydrazone was included to increase permeability to H^+ that is ejected during Ca^{2+} uptake. Random insertion of pump units was confirmed by 2-fold activation of ATPase activity following solubilization in $C_{12}E_8$, and that rates of transport were approximately half that in native SR vesicles, where 100% of units are physiologically orientated (cytoplasmic surface outwards). The effects of lipid composition on Ca^{2+} uptake, using Arsenazo III, and ATPase activity in proteoliposomes were determined. Slippage was defined as the process in which the phosphorylated intermediate releases bound Ca^{2+} on the cytoplasmic, rather than on the lumenal side of the membrane. Kinetics of Ca^{2+} uptake can distinguish contributions of slippage and leakage, by comparison with simulation of the reaction mechanism.

In the absence of anionic phospholipid (100% dioleoylphosphatidylcholine (DOPC)), the slippage rate of the reaction $E_2\text{-}P.Ca_2 \rightarrow E_2\text{-}P + 2Ca^{2+}_{out}$ was 250 s^{-1}. Slippage was 65 s^{-1} in controls and zero with either 10 mol% dioleoylphosphatidic acid or cardiolipin. Slippage with 10% PtIns(4)P was 15 s^{-1}. It is of note that the optimal concentration of anionic phospholipid of 10 mol% is the same as the mol fraction in native SR [155,156].

Chain lengths of phospholipid also affect catalysis by the Ca^{2+}-ATPase. Optimum conditions for ATPase activity of reconstituted vesicles are DOPC (di(C18:1)PC). Longer or shorter chain lengths give lower activity. Two Ca^{2+} ions bind per mol ATPase, as in the native state. However, when membrane lipid is changed to dimyristoleoylphosphatidylcholine, (C14:1)PC, the stoichiometry changes to one Ca^{2+} ion per ATPase [157]. Further characterization [29] showed that chain lengths of C12, C14 or C24 also resulted in binding of one Ca^{2+} per monomer. The change of one to two sites with mixtures of phospholipid shows high cooperativity with respect to membrane composition, suggesting multiple lipid/protein contact sites that can influence protein conformation. With two Ca^{2+} sites, binding at the second site blocks release from the deeper site. Under conditions that support one Ca^{2+} site there is minimal effect of medium Ca^{2+} on Ca^{2+} release. The mechanism of the effects of phospholipids on Ca^{2+} binding sites is unknown, but it has been suggested that chain lengths of phospholipids of between C16 and C22 are required to prevent the outer gate from closing with only one ion bound in the channel [29].

The two contrasting effects of phospholipids are illustrative. Chain length causes changes in stoichiometry, whilst anionic phospholipids decrease slippage.

7.4. *Slippage of the Ca^{2+}-ATPase at limiting $[Ca^{2+}]_{out}$*

We now consider another condition, limiting Ca^{2+}_{out}, or $[Ca^{2+}]_{lim}$, where the Ca^{2+}-ATPase activity is limited kinetically by low external $[Ca^{2+}]$ in a mechanism with emptied (unfilled) Ca^{2+} uptake sites. This is not the equivalent of 'level flow' where the pump has maximum access to transported species against zero back pressure. The key question is can the Ca^{2+}-ATPase turnover without binding of Ca^{2+} to high affinity cytosolic sites.

Coupling ratios, Ca^{2+}/ATP, have been measured previously using independent steady state assays of Ca^{2+} transport, with $^{45}Ca^{2+}$ or spectrophotometric Ca^{2+} probes, and of ATPase activity, either by $^{32}P_i$ release from [γ-^{32}P]ATP or by a NADH-coupled assay. Earlier studies typically gave coupling ratios between 1.5 and 2.0 under optimal conditions. Failure to achieve values of 2.0 was generally assumed to be due to leakage pathways, or that some SR vesicles were not sealed. This approach appeared to be valid since it is as predicted by a rigid single catalytic cycle.

The effects of $[Ca^{2+}]_{out}$ on coupling ratios may be determined using Ca^{2+}/EGTA buffers, and measured in the linear phase of the steady state. One of the uncertainties is the nature of ATPase activity at low levels ($\leq 10^{-7}$ M) of $[Ca^{2+}]_{out}$, referred to as Mg^{2+}-ATPase or 'basal' ATPase. The general consensus is that this activity is due to an independent ATPase, probably derived from plasma or T-tubule, in which case it may be subtracted from 'total' ATPase to give the true Ca^{2+}-dependent ATPase activity. There are differences between Mg^{2+}- and Ca^{2+}-ATPase, apart from Ca^{2+} sensitivity. The K_d for ATP is in the millimolar range [158], compared to the micromolar

Ca^{2+}-ATPase site. Furthermore Mg^{2+}-ATPase is abolished in detergent, whereas Ca^{2+}-ATPase activity may be increased [159]. 'Basal' Mg^{2+}-ATPase activity in the absence of Ca^{2+} is, however, not inhibited by TG (unpublished observation). It is possible that the TG.E_1 complex is able to turn over at <2–5% of V_{max}.

Alternate methods of measuring coupling ratios, based on pulsed additions of either ATP or Ca^{2+}, allow determination of Ca^{2+}/ATP at μM ATP, whilst Ca^{2+}-stat methods can determine coupling ratios in the submicromolar Ca^{2+} levels [160]. Ca^{2+}/ATP ratios of 1.82 and 1.79 were obtained by the ATP- and Ca^{2+}-pulse methods respectively. The advantage of ATP-pulsed methods, where [ATP] does not exceed 20 μM, minimizes the contribution of Mg^{2+}-ATPase activity. Ca^{2+}/ATP ratios varied from 0.1 at 0.05 μM Ca^{2+} to a maximum of 1.8 from 1–30 μM Ca^{2+} [161]. Correction for Mg^{2+}-ATPase at 0.075 μM Ca^{2+} altered the estimated ratio from 0.44 to 0.49. The Ca^{2+} dependency of coupling could be fitted to a relationship with $Ca^{2+}/ATP = 1.8$, $[Ca^{2+}]_{0.5} = 0.12 \pm 0.03$ μM, and $n_{H(Ca^{2+})} = 2.0 \pm 0.4$. These parameters are similar to those of Ca^{2+} binding, and of Ca^{2+} stimulation of transport and ATPase activities [162–164], although Ca^{2+} dependence of kinetic effects may not necessarily follow those of binding studies.

Low stoichiometries occur at alkaline pH and at high temperatures [165–168]. Ratios are near maximum at pH 6.8 and decline to near zero at pH 7.9. This is unlike a membrane lipid pathway for efflux, which has no pK_a of phospholipid headgroups in this range. In addition, the permeability of purified lipid bilayers to Ca^{2+} is low [169], and is somewhat increased by insertion of the Ca^{2+}-ATPase into the lipid membrane [26]. The main pathway for leakage in native SR vesicles is also via the pump protein [26,170–172], which explains why leakage is blocked by μM Ca^{2+} [27,173]. Exchange of $^{45}Ca^{2+}$ at maximum loading of 200–400 nmol/min/mg [174] is 10-fold greater than passive efflux of 20–60 nmol/min/mg [172,175]. Exchange of $^{45}Ca^{2+}$ under maximally loaded conditions occurs via the Ca^{2+}-ATPase with minimal amounts through 'lipid channels' [176]. Thus many lines of evidence concur that passive leakage via non-specific lipid permeability cannot account for the observed sub-stoichiometric coupling ratios, and that back diffusion via a channel within the Ca^{2+}-ATPase accounts for the phenomenon of slippage.

The data reviewed here concur that coupling of transport to enzyme turnover is markedly decreased at $[Ca^{2+}]_{free}$ levels below 1 μM, and becomes near zero (0.1) at 50 nM. It appears that the Ca^{2+}-ATPase can turnover with both Ca^{2+} binding sites vacant. This raises the question again that Mg^{2+}-ATPase activity may be an alternate catalytic pathway that is favored in the absence of Ca^{2+}. Support for this concept is that the Mg-ATPase activity of rat cardiac SR also is a function of Ca^{2+}-ATPase protein [177].

7.5. Mechanism of uncoupled UTP hydrolysis

A number of non-physiological substrates support transport by SR, including AcP [144,178], *p*-nitrophenylphosphate, methylumbelliferylphosphate and dinitrophenylphosphate [139], and give coupling ratios near 1.0. Ratios of 2.0 have been reported for UTP and other pseudo-substrates [179,180]. Intramolecular uncoupling of ATP-supported Ca^{2+} transport has been linked to phosphorylated intermediates with dissociation of Ca^{2+} to the cytoplasmic surface [97,161]. However, it has also been suggested that rapid efflux of Ca^{2+} might proceed via cycling of non-phosphorylated intermediates [103,178]. A problem when investigating coupling and uncoupling with ATP as substrate is that there are complex effects on several steps of the catalytic cycle. UTP appears to have a more clear cut role as substrate since it does not support rapid Ca_{cyt}–Ca_{lum} exchange.

The uncoupling mechanism of the Ca^{2+}-ATPase of SR has been investigated by Fortea et al. [181], using UTP as substrate. High levels of lumenal Ca^{2+} do not affect UTP hydrolysis, but do limit Ca^{2+} transport and net uptake of Ca^{2+} decreases with Ca^{2+} preloading. In unloaded SR vesicles coupling ratios decline from 1.0 to 0.6 within 6 s. There is some concern with selection of parameters for calculating the amounts of substrate used per Ca^{2+} transported, since there is appreciable 'basal' ATPase activity in the presence of EGTA. This problem is not a major factor with ATP as substrate, where Ca^{2+}-independent hydrolysis is only a small fraction of total ATPase activity. With UTP, however, Ca^{2+}-independent activity contributes 55% of the total UTPase activity. Unlike the case with ATP, this 'basal' activity in-

volves a phosphorylated intermediate that has identical electrophoretic mobility to that of Ca^{2+}-dependent E-P formation [181]. Oxalate promotes a longer time of linear uptake with a coupling ratio of 0.7 with UTP, which is independent of time.

The nature of E-P species present during uncoupled UTP hydrolysis is of special interest. Steady state levels of total E-P in the uncoupled state (high lumenal Ca^{2+}) were 3.7 nmol/mg (approximately 1 mol/mol enzyme). No superfluorescence of TNP-ATP, which monitors E_2-P intermediates [89], occurred with uncoupling. When turnover was slowed at pH 8.0, and with K^+ and oxalate, E-P was 4.8 nmol/mg, and there was a marked increase in TNP-ATP superfluorescence, indicating predominant accumulation of E_2-P. It can be concluded that with UTP E_1-P.Ca_2 accumulates in the steady state under uncoupling conditions. A question that arises is of the fate of Ca^{2+} bound as E_1-P·Ca_2 during uncoupled UTP hydrolysis. Ca^{2+} that is bound to the enzyme cannot be exchanged with external (cytoplasmic) medium, whereas EGTA displaced 9 nmol/mg (2 mol/mol ATPase).

Further insight into the nature of turnover in the uncoupled state was obtained from the effects of the high affinity inhibitor, cyclopazonic acid (CPA). CPA inhibited UTP hydrolysis in the presence of the Ca^{2+} ionophore, A23187, but had no effect in its absence. Since CPA is known to bind to E_2 [182] this suggests that E_2-P is not the main form of E-P in the uncoupled state, and that its hydrolysis proceeds via E_1-P·Ca_2.

Three independent measurements support the proposed model by Fortea et al. [181]: (1) E_2-P in uncoupled vesicles is absent in the steady state. (2) Ca^{2+} dissociates from E_1-P.Ca_2 to the cytoplasmic surface in the coupled state, but not in the first few turnovers before vesicles are filled with Ca^{2+} [98]. (3) CPA, a specific E_2 binding inhibitor [182], did not affect UTP hydrolysis in the uncoupled state, but did so with A23187, which promoted forward operation of the pump via E_2.

ATP and UTP both form E_1-P.Ca_2 as part of their catalytic cycles. The question arises as to why ATP favors a coupled cycle, whereas that from UTP is uncoupled with high $[Ca^{2+}]_{lum}$. One simple explanation is that the step E_1-P.$Ca_2 \rightarrow E_2$-P.Ca_2 is known to be accelerated by ATP and not by UTP [183,184].

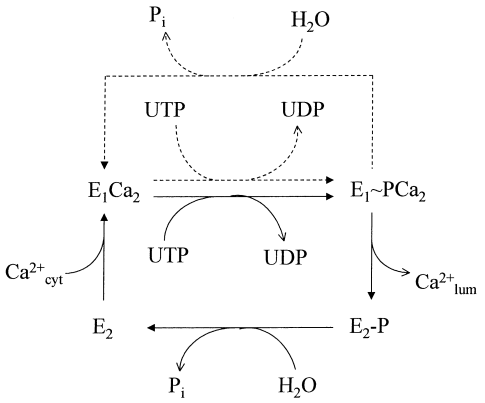

Fig. 4. Coupled and uncoupled cycles of UTP hydrolysis by the Ca^{2+}-ATPase of SR (Fortea et al., [181]).

With ATP as substrate, and with Ca^{2+}-loaded vesicles both E_1-P.Ca_2 and E_2-P.Ca_2 accumulate and are difficult to study due to $^{40}Ca^{2+}$–$^{45}Ca^{2+}$ exchange [185,186].

A simple reaction scheme, shown in Fig. 4, has been used to explain the interaction of coupled and uncoupled cycles of the Ca^{2+}-ATPase with UTP as substrate [181]. The first committed step of the uncoupled path is the hydrolysis of E_1-P.Ca_2 with the release of P_i. This is followed by the release of two Ca^{2+} to the cytoplasmic medium. The coupled cycle is favored by ATP binding to a low affinity but highly specific regulatory site that leads to E_2-P.2Ca.

8. Turnover of the Na^+/K^+-ATPase in the absence of K^+

Under optimal conditions red blood cell Na^+/K^+-ATPase turns over with a Na:K:ATP ratio of 3:2:1. However, in the absence of K^+, the pump catalyzes at least three ATP-dependent activities. These include Na^+–Na^+ exchange [187–191], uncoupled Na^+ efflux [192,193] and ATP-dependent Na^+ efflux [194,195]. Na^+ replaces K^+ as a surrogate to facilitate turnover. Three distinct species of E-P have been defined as intermediates of the Na^+/K^+-ATPase cycle on the basis of ADP and K^+ sensitivity [196]. E_1-P is ADP-sensitive and K^+-insensitive, while E_2-P is ADP-insensitive and K^+-sensitive. The fact that the sum of E_1-P and E_2-P was 150% of total E-P lead Yoda and Yoda [196] to propose the existence of a third species E*P that is both ADP- and K^+-

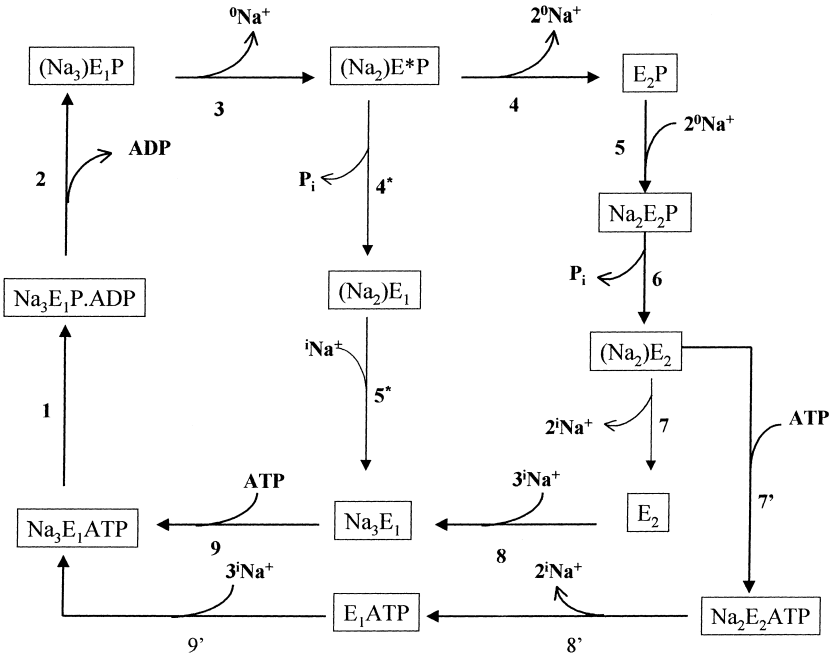

Fig. 5. Multiple branched cycles of the red blood cell Na^+/K^+-ATPase in the absence of K^+ (Yoda and Yoda, [198]).

sensitive. The conversion $E_1 \rightarrow E_1$-P is faster than $E_1 \rightarrow E^*P$, and $E^*P \rightarrow E_2$-P is slower than E_1-P $\rightarrow E^*P$. Distribution of each species depends on $[Na^+]$; E_1-P predominates at 400 mM Na^+, E*P at 60–300 mM, and E_2-P at < 60 mM. The distribution of E-Ps also depends on the cholesterol content of reconstituted proteoliposomes [197], in particular, high cholesterol phospholipid (HCPL) mixtures favor E*P, whilst low cholesterol phospholipid (LCPL) favors E_2-P. The main component in HCPL dephosphorylates through a pathway different from that of E_2-P [198]. Further evidence for separate pathways is that their stoichiometries are different. With HCPL (E*P) coupling ratios are 1.6:0.6:1, whilst with LCPL they are 2.8:1.8:1. Ionophores, monensin and A23187, increased Na^+ influx:ATP from 1.4:1 to 2.8:1 for E*P and E_2-P cycles respectively. The E_2-P cycle is analogous to ATP-dependent Na^+–Na^+ exchange in red blood cells [194,195] and in proteoliposomes [199]. In the LCPL cycle ATPase and Na^+ influx are enhanced by low affinity binding. Similar stimulation of HCLP activity by ATP only occurs in the presence of ionophore monensin or A23187, indicating that the reaction $E_2 \rightarrow E_1$ is included in the E_2-P cycle but not in the E*P cycle.

A reaction scheme (Fig. 5) [198] shows three possible cycles or pathways for Na^+ transport in proteoliposomes in the absence of K^+. The E_2-P pathway is the fully coupled cycle shown in Fig. 1. At low ATP the pathway through intermediates 1–9 results in stoichiometries of 3:2:1 for Na^+:Na^+:ATP. High [ATP] favors reactions $1 \rightarrow 6 \rightarrow 7' \rightarrow 8' \rightarrow 9$, with similar coupling ratios. The E*P cycle $1 \rightarrow 3 \rightarrow 4^* \rightarrow 5^* \rightarrow 9$ transports one of the three occluded Na^+ in E_1-P(Na_3), and the two Na^+ in E*P(Na_2) remain occluded, and E*P and E_2-P have similar conformations. Binding of intravesicular Na^+ to E_2-P stimulates its hydrolysis [195]. The step $E_2 \rightarrow E_1$ is the slow step that is accelerated by ATP binding to the low affinity site. High ATP does not stimulate hydrolysis by the HCPL enzyme and the conformational change $E_1 \rightarrow E_2$ is not included in the E*P cycle, since the E*P cycle is only observed when $E^*P \rightarrow E_2$-P is inhibited by high cholesterol in HCPL.

The findings of Yoda and Yoda [196–198] have relevance for the choice of suitable models that have been proposed for the mechanism of energy coupling in the Na^+/K^+-ATPase. Firstly, they demonstrate that there are at least three possible species of E-P that form part of the sequence for energy transduction in the fully coupled state that can be observed with manipulation of the lipid composition of PLs. Secondly, branched cycles are possible under

conditions that might occur in vivo. Overlapping cycles are required to explain the behavior, at least in reconstituted PLs. Furthermore, the branch point has been identified at E_1-P.3Na. Most significantly, binding of ATP to a low affinity regulatory site directs flux through the cycle that is optimally coupled. Lastly there can be little doubt that the Na^+/K^+-ATPase can be expected to pursue an uncoupled pathway under conditions that may occur pathologically, and dissipate ATP whilst conserving fluxes of Na^+ and K^+.

Under fully saturated ionic conditions, pig kidney Na^+/K^+-ATPase, reconstituted into PLs, transport reaches 3:2:1 for Na^+:K^+:ATP flux ratios. This transport is electrogenic and gives rise to membrane potentials of up to 250 mV that can be readily determined with Oxonal VI [200]. This confirms findings that pump-mediated current is one-third of active Na^+ flux.

Goldshleger et al. [200] have determined the electrogenicity of the Na^+/K^+-ATPase, incorporated into PL vesicles, including two types of Na^+–Na^+ exchange, and of 'uncoupled' Na^+ flux, which is the ATP-dependent uptake of Na^+ into PL vesicles in the absence of K^+. 'Uncoupled' Na^+ flux occurs typically at 1% of the rate of Na^+/K^+ exchange [201,202]. Comparison of initial rates of steady state potentials with ATP-dependent ^{22}Na fluxes into K^+-loaded vesicles, with Na_{cyt} = 2–50 mM, [ATP] = 1–1000 μM and pH 6.5–8.5, gave optimal coupling ratios. However if $[Na]_{cyt}$ is <0.8 mM, coupling ratios less than optimum were obtained.

'Uncoupled' Na^+ flux is electroneutral at pH 6.5–7.0, due to neutral $3Na_{cyt}/3H_{exc}$ exchange, but reaches $3Na_{cyt}$/no ions at pH 8.5. These findings lead to the general conclusion that for the Na^+/K^+-ATPase coupling ratios are maximal and fixed when transport sites are saturated, but at low concentrations of the transported ions, e.g. Na_{cyt} in Na/K exchange and H^+_{exc} in 'uncoupled' Na^+ flux, coupling ratios may decrease.

9. Uncoupling and slippage of P-type pumps and regulation of metabolism

The SERCAs and Na^+/K^+-ATPase together are significant ATP consuming processes that contribute to energy utilization in mammals (for review see [203] and references therein). In particular the Na^+/K^+-ATPase accounts for 20% of the standard metabolic rate (SMR), being highest in brain and kidney, where the pump is coupled to 50–60% of O_2 consumption. The Ca^{2+}-ATPase accounts for 6% of SMR metabolic rate in resting muscle and up to 24–58% during maximal contraction (for review see [204]).

The consensus is that SMR is due to extramolecular uncoupling reactions; ion channels in brain, Na^+ channels and Na^+-coupled transport, Na^+ reabsorption in kidney, and opening of Ca^{2+} channels in muscle. Likewise, gluconeogenesis is effectively uncoupled by glycolysis. Of overall ATP production 19–28% is consumed by Na^+/K^+-ATPase activity, and 4–8% by the Ca^{2+}-ATPase. During non-shortening muscle activity relative ATP consumption is due to actomyosin, 65–80%, and 10–25% by Ca^{2+}-ATPase. Ca^{2+} cycling may require 20–50% of ATP turnover in shortening muscle [204,205].

Rolfe and Brown [203] have concluded that '...it is important to consider which reactions uncouple these processes, since without the uncoupling reactions there would be no SMR'. In these instances the coupling reactions are performed by different physical systems to the primary mechanisms and are thus uncoupled 'extramolecular' reactions. We may therefore consider if there is any evidence for an 'intramolecular' type of uncoupling that might give rise to extra heat production in, for example, non-shivering thermogenesis (NST).

Energy consuming ATPases are relatively inefficient. The Na^+/K^+-ATPase evolves 15 kJ/mol. Assuming that $\Delta\Psi$ is 60 mV [206–208], and that the enthalpy equivalent of ATP hydrolysis is 21 kJ/mol, means that the equivalent of one charge transfer is 6 kJ/mol. In brain, ΔGATP is 62 kJ/mol and only 35 kJ/mol is transferred to Na^+ and K^+ gradients, and $\Delta\Psi$, giving an efficiency of 57%. The plasma membrane Ca^{2+}-ATPase has an efficiency of 42%, based on an ATP:Ca^{2+}:H^+ stoichiometry of 1:1:2 and plasma membrane $\Delta G(Ca^{2+})$ of 26 kJ/mol [209].

9.1. Heat production by the Ca^{2+}-ATPase of skeletal muscle SR

It has been established that a major source of heat during NST is derived from resting skeletal muscle

[210]. It has been assumed that ATP hydrolysis is needed to transport Ca^{2+} back into SR, which leaks out by unspecified pathways. In other terms part of the energy derived from ATP hydrolysis is required for transport and the rest is released as heat.

De Meis and colleagues have made direct in vitro measurements of heat produced by isolated SR vesicles, using microcalorimetry [211]. They found that the amount of energy released per mol of ATP hydrolyzed depended upon formation of a Ca^{2+} gradient. In intact vesicles (high gradient) −93 kJ/mol of heat was released, which was greater than that with leaky vesicles (no gradient) of −51 kJ/mol, suggesting that part of the osmotic energy could be released by efflux of Ca^{2+}, uncoupled from ATP synthesis, which is endergonic. Reagents that modified the degree of coupling of Ca^{2+} efflux to ATP synthesis resulted in differences in heat released. Heparin, which blocks Ca^{2+} transport, increased ΔH^{cal} from −93 to −126 kJ/mol. DMSO, 20%, which enhanced Ca^{2+} uptake, decreased ΔH^{cal} to −55 kJ/mol. It appears that accumulated Ca^{2+} can either exit through the Ca^{2+}-ATPase and synthesize ATP, or result in uncoupled efflux via the ATPase with release of extra heat. In the absence of a Ca^{2+} gradient, high (mM) [Ca^{2+}] causes some of the energy, derived from ATP hydrolysis, to be used to resynthesize ATP, and a smaller fraction is dissipated as heat [212]. Thus ΔH^{cal} for ATP hydrolysis can vary from $\cong$10 to 126 kJ/mol, depending upon the degree of coupling of the Ca^{2+} pump. Simultaneous measurements of Ca^{2+} efflux, heat production and ATP synthesis from ADP and P_i showed that the Ca^{2+}-ATPase can perform three different reactions, all of which are inhibited by the specific inhibitor, TG: (i) heat absorption of 21 kJ/mol Ca^{2+} during ATP synthesis; (ii) release of 126 kJ/mol when Mg^{2+} is removed to abolish ATP synthesis; and (iii) no heat production when ligands of the enzyme are removed from the medium [213].

9.2. Ocular heater organ in Billfish

One of the most unique heat organs is present in the extraocular muscles of ocean Billfish, such as Marlin and Swordfish [210,214–216]. The superior rectus muscles are highly differentiated and contain no contractile elements. These heater cells are packed with mitochondria and smooth membranes, which are covered with Ca^{2+}-ATPase pump units, and function to keep the brain tissue of these poikilotherms warm during long dives in cold ocean environments. It is generally assumed that mitochondria are a source of ATP, which is hydrolyzed by the Ca^{2+}-ATPase, due to extramolecular uncoupling by open Ca^{2+} channels, analogous to the ryanodine channel in skeletal muscle. Logically, thermogenesis may be activated in excitation–contraction coupling and depolarization of T-tubules by action potentials derived from plasma membrane. The precise channels of Ca^{2+} release are, however, not known, and there is the possibility that intramolecular uncoupling or slippage may be responsible for collapse of the Ca^{2+} gradient within the SR lumen, necessary for maintaining the SR as an ATP consuming process.

10. Slippage and uncoupling of the Ca^{2+}-ATPase in ageing and disease

Instability of Ca^{2+} transport, and relative stability of ATP hydrolysis, leading to uncoupling of SR vesicles under relatively mild conditions, might be encountered under extremes of physiological states or in disease.

As discussed previously, under near physiological conditions, like EGTA at 37°C, uncoupling of the Ca^{2+}-ATPase occurs within the minute time scale, which leads to the question why does uncoupling not occur in vivo, and could uncoupling be a feature of ageing?

Transport rates by SR vesicles, prepared from slow twitch soleus muscle of aged rats, were 50% lower than that from adults [217]. This is due to a decrease in V_{max} and an increase in $K_{0.5(Ca)}$. ATPase activities were unaffected. Relaxation time of intact muscle, after isometric force, which is dependent on Ca^{2+} reuptake rates, was significantly prolonged in aged preparations. Effects were muscle-specific as no similar ageing effects were seen in fast twitch gastrocnemius muscle. The ageing process has been correlated with nitration by peroxynitrite ($ONOO^-$) to the sequence Tyr294–Tyr295 in the M4–M8 transmembrane domain of SERCA2a [218]. In addition, conformational stability of the Ca^{2+}-ATPase was altered in ageing muscle. Incubation of SR ATPase at 37°C

resulted in more rapid inactivation of transport from aged vesicles compared to those from young adult rats [219]. Aged SR vesicle Ca^{2+}-ATPase was more susceptible to tryptic digestion, suggesting that increased exposure of hydrophobic segments is the basis of critical loss of conformational and functional stability.

Global ischemia of rat whole brain preparations leads to loss of cytosolic Ca^{2+} homeostasis, and of decreased Ca^{2+} uptake into endoplasmic reticulum vesicles [220]. Ischemia for 5–60 min had no effect on TG-sensitive ATPase activity. Ischemia therefore causes irreversible uncoupling of brain microsomal Ca^{2+} cycling.

Defibrillation by high voltage shocks, applied to the thorax, is the standard procedure for treatment of ventricular fibrillation. Following a series of 10 shocks in rats, isolated cardiac SR vesicles showed a decrease in Ca^{2+} transport without effects on ATP hydrolysis [221]. This finding would suggest that irreversible intramolecular uncoupling might be the basis of the unexplained diminished cardiac contractility that follows successful reversal of fibrillation.

The effects of ischemia on sarcolemmal vesicles prepared from rabbit hearts have been compared to controls [222]. One hour of ischemia caused a 26% increase in Na^+/K^+-ATPase. Na^+ pumping was decreased from 2.4 to 1.1 nmol/mg/s. These findings explain the loss of K^+ and accumulation of Na^+ by ischemic myocardial cells.

Uncoupling of P-type ATPases appears to be an important mechanism of organ dysfunction in some common clinical conditions.

11. Periodic forcing of a Brownian particle

During investigations of possible mechanisms for active transport it was considered helpful to seek some readily analyzed physical model on which further experimental approaches to the problem of energy transduction in the P-type ATPases might be based. Basically we are considering a molecular motor operating in a fairly rigid fixed channel, in which complex conformational changes are linked to 'uphill' transport of cations. Reverse flux of cation should be minimized, i.e. the Ca^{2+} current is rectified. Such a model should incorporate a multisite

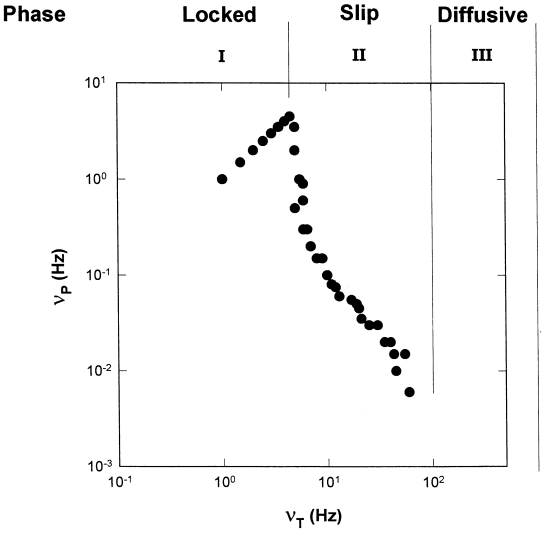

Fig. 6. Correlation of cyclic rotation of a laser optical trap, ν_T, with movements of a dielectric particle, ν_P, undergoing Brownian motion (Faucheux et al., [223]).

channel with cations 'hopping' according to a stochastic process. Models should incorporate the phenomena of tight coupling, slippage and passive cation-specific flux.

One such model has been investigated by Faucheux et al. [223], who analyzed movements of a particle in a circular planar field. The experimental system consists of a laser beam that acts as an optical 'tweezer', which creates an inhomogeneous intensity profile that traps a 2 μm polystyrene dielectric particle in a rotating field. Movement of the particle depends on viscous drag (Stokes force), proportional to velocity. The laser trap is constrained to rotate in a 12.4 μm diameter circle.

Below 100 μm/s (5 Hz), the particle faithfully follows the optical trap in a phase-locked manner (Fig. 6). At a critical frequency of 5 Hz the trap is not strong enough to hold the particle, but it receives a 'kick' during each cycle, such that the particle revolves at $\nu_P < \nu_T$ in a phase slip regime, where ν_T and ν_P are the trap and particle angular frequencies respectively. Just above the critical frequency there is a sharp decrease in ν_P and the system effectively slips. Direct observation showed that the particle behaved in a stochastic manner, in the slippage regime, varying from a complete revolution to near zero. At still higher frequencies $\nu_P \rightarrow 0$, and the system attains a diffusive regime. One important characteristic of

this state is that the particle is constrained to diffuse along the circle.

It is tempting to suggest that phase 'locked', 'slip' and 'diffusive' regimes correspond to coupled transport, slippage and passive diffusion properties of the P-type cation pumps.

12. Conclusions

This review has focused on different approaches that have been employed to determine those events that result in coupling of scalar and vectorial events during energy transduction in well documented P-type ATPases, the SERCA Ca^{2+}-ATPase and plasmalemmal Na^+/K^+-ATPase and H^+-ATPase. There are a number of examples that lead to uncoupling or slippage. A key reaction is at the branch point E_1-P with bound cations. Isomerization to E_2-P is the event that determines the fate of the occluded cation. Conditions that lead to the accumulation of E_1-P result in uncoupled release of cations to the *cis* (cytoplasmic) surface.

There is evidence that transport occurs in a limited channel within the ATPase that is cation-specific. Occluded cations are an intermediate species within the channel. Failure to form occluded cations is a common feature of the uncoupled state. Partial thermal denaturation, which results in uncoupling, also blocks formation of occluded cations. Slippage appears to be an inherent property of P-type pumps, and is not an artefact.

The crystal structure of the Ca^{2+}-ATPase at 2.8 Å is in agreement with the general proposals for the structure of the Ca^{2+}-ATPase based on more indirect evidence. Crystals of the enzyme, formed in the presence of high [Ca^{2+}], only show two side-by-side Ca^{2+} ions. Kinetic studies suggest that there are a total of four or possibly six sites within the channel.

In terms of more general biological importance, slippage is not a trivial event. It involves at least two of the major energy consuming processes in mammalian metabolism. Slippage has also been utilized for heat production.

Finally, several instances of common disease processes, such as ageing and cardiac failure, are examples of the role of uncoupling in the pathogenesis of the disease state. Hopefully further studies will reveal details of the transduction mechanism, and suggest rational therapy for those conditions in which uncoupling or slippage has been shown to play a part.

Acknowledgements

I wish to acknowledge expert technical assistance of Abduraman Mohammed, and stimulating discussions with Prof. David McIntosh. This work was supported by grants from the Harry Crossley and Staff Research Funds of the University of Cape Town.

References

[1] P. Mitchell, Science 206 (1979) 1148–1159.
[2] P. Mitchell, Trans. Biochem. Soc. 4 (1976) 399–430.
[3] S. Ebashi, F. Lippman, J. Cell Biol. 14 (1962) 389–400.
[4] W. Hasselbach, M. Makinose, Biochem. Z. 339 (1963) 94–111.
[5] L. De Meis, A.L. Vianna, Annu. Rev. Biochem. 48 (1979) 275–292.
[6] I.M. Glynn, S.J.D. Karlish, Annu. Rev. Biochem. 59 (1990) 171–205.
[7] C. Tanford, Annu. Rev. Biochem. 52 (1983) 379–409.
[8] P. Lauger, Biochim. Biophys. Acta 552 (1979) 143–161.
[9] W. Hasselbach, H. Oetliker, Ann. N.Y. Acad. Sci. 402 (1983) 459–469.
[10] C.S. Patlak, Bull. Math. Biophys. 19 (1957) 209–235.
[11] G.A. Vidavar, J. Theor. Biol. 10 (1966) 301–306.
[12] O. Jardetsky, Nature 211 (1966) 969–970.
[13] A. Dutton, E.D. Rees, S.J. Singer, Proc. Natl. Acad. Sci. USA 73 (1976) 1532–1536.
[14] M. Klingenberg, Nature 290 (1981) 449–454.
[15] J. Kyte, Nature 292 (1981) 201–204.
[16] C. Tanford, Proc. Natl. Acad. Sci. USA 80 (1983) 3701–3705.
[17] M.L. Jennings, in: N. Hamasaki, M.L. Jennings (Eds.), Anion Transport Protein of the Red Blood Cell Membrane, Elsevier, Amsterdam, 1989, pp. 59–72.
[18] D.C. Gadsby, R.F. Rakowski, P. De Weer, Science 260 (1993) 100–103.
[19] P. Lauger, Electrogenic Ion Pumps, Sinauer Associates, Sunderland, MA, 1991.
[20] P. Mitchell, J. Moyle, Biochem. Soc. Spec. Publ. 4 (1974) 91–111.
[21] C.L. Slayman, D. Sanders, Biochem. Soc. Symp. 50 (1985) 11–29.
[22] A. Su, S. Mager, S.L. Mayo, H.A. Lester, Biophys. J. 70 (1996) 762–777.
[23] P.G. Stein, P.T. Palade, Biophys. J. 54 (1988) 357–363.

[24] J. Wang, J.M. Tang, R.S. Eisenberg, J. Membr. Biol. 130 (1992) 163–181.
[25] G. Inesi, M.E. Kirtley, J. Membr. Biol. 116 (1990) 1–8.
[26] R.L. Jilka, A.N. Martonosi, T.W. Tillack, J. Biol. Chem. 250 (1975) 7511–7524.
[27] R.L. Jilka, A.N. Martonosi, Biochim. Biophys. Acta 466 (1977) 57–67.
[28] M.C. Berman, Biochim. Biophys. Acta 694 (1982) 95–121.
[29] A.P. Starling, J.M. East, A.G. Lee, Biochemistry 32 (1993) 1593–1600.
[30] W.P. Jencks, J. Biol. Chem. 264 (1989) 18855–18858.
[31] M.C. Berman, D.B. McIntosh, J.E. Kench, J. Biol. Chem. 252 (1977) 994–1001.
[32] D.B. McIntosh, M.C. Berman, J. Biol. Chem. 253 (1978) 5140–5146.
[33] D.H. MacLennan, W.J. Rice, N.M. Green, J. Biol. Chem. 272 (1997) 28815–28818.
[34] G. Inesi, L. De Meis, J. Biol. Chem. 264 (1989) 5929–5936.
[35] H. Rottenberg, Proc. Natl. Acad. Sci. USA 80 (1983) 3313–3317.
[36] J. Nakamura, J. Biol. Chem. 269 (1994) 30822–30827.
[37] D. Pietrobon, M. Zoratti, G.F. Azzone, S.R. Caplan, Biochemistry 25 (1986) 767–775.
[38] D.B. McIntosh, Adv. Mol. Cell. Biol. 23A (1998) 33–99.
[39] C.J. Brandl, S. deLeon, D.R. Martin, D.H. MacLennan, J. Biol. Chem. 262 (1987) 3768–3774.
[40] H. Ogawa, D. Stokes, H. Sasabe, C. Toyoshima, Biophys. J. 75 (1998) 41–52.
[41] D.M. Clark, T.W. Loo, G. Inesi, D.H. MacLennan, Nature 339 (1989) 476–478.
[42] C. Toyoshima, M. Nakasako, H. Nomura, H. Ogawa, Nature 405 (2000) 647–655.
[43] D.J. Bigelow, T.C. Squier, G. Inesi, J. Biol. Chem. 267 (1992) 6952–6962.
[44] D.H. MacLennan, C.J. Brandt, B. Korczak, N.M. Green, Nature (Lond.) 316 (1985) 696–700.
[45] M. Nayal, E. Di Cera, Proc. Natl. Acad. Sci. USA 91 (1994) 817–821.
[46] J.V. Moller, B. Juul, M. le Maire, Biochim. Biophys. Acta 1286 (1996) 1–31.
[47] G. Inesi, M. Kurzmack, C. Coan, D.E. Lewis, J. Biol. Chem. 255 (1980) 3025–3031.
[48] D.A. Doyle et al., Science 280 (1998) 69–77.
[49] G. Inesi, J. Biol. Chem. 262 (1987) 16338–16342.
[50] V. Forge, E. Mintz, D. Canet, F. Guillain, J. Biol. Chem. 270 (1995) 18271–18276.
[51] D. Canet, V. Forge, F. Guillain, E. Mintz, J. Biol. Chem. 271 (1996) 20566–20572.
[52] M.C. Berman, Biochim. Biophys. Acta 1509 (2000) 42–54.
[53] E.H. serpersu, U. Kirch, W. Schoner, Eur. J. Biochem. 122 (1982) 347–354.
[54] B. Vilsen, J.P. Andersen, Biochim. Biophys. Acta 855 (1986) 429–431.
[55] M. Kurzmack, G. Inesi, FEBS Lett. 74 (1977) 35–37.
[56] S. Verjovski-Almeida, M. Kurzmack, G. Inesi, Biochemistry 17 (1978) 5006–5013.
[57] Y. Dupont, Eur. J. Biochem. 109 (1980) 231–238.
[58] Y. Yakakuwa, Y. Kanazawa, Biochem. Biophys. Res. Commun. 88 (1978) 1209–1216.
[59] W. Waas, W. Hasselbach, Eur. J. Biochem. 116 (1981) 601–618.
[60] B. Vilsen, J.P. Andersen, Biochim. Biophys. Acta 898 (1987) 313–322.
[61] H. Takisawa, M. Makinose, J. Biol. Chem. 256 (1983) 2986–2992.
[62] M.C. Berman, Biochim. Biophys. Acta 1418 (1999) 48–60.
[63] M. Wictome, Y.M. Khan, J.M. East, A.G. Lee, Biochem. J. 310 (1995) 859–868.
[64] I.M. Glynn, J.F. Hoffman, J. Physiol. 218 (1971) 238–256.
[65] I.M. Glynn, D.E. Richards, Curr. Top. Membr. Transp. 19 (1983) 625–638.
[66] I.M. Glynn, Y. Hara, D.E. Richards, J. Physiol. 351 (1984) 531–547.
[67] S.J.D. Karlish, D.W. Yates, Biochim. Biophys. Acta 527 (1978) 115–130.
[68] I.M. Glynn, S.J.D. Karlish, Annu. Rev. Biochem. 59 (1990) 171–205.
[69] R.L. Post, C. Hegyvary, S. Kume, J. Biol. Chem. 247 (1972) 6530–6540.
[70] S.J.D. Karlish, D.W. Yates, I.M. Glynn, Biochim. Biophys. Acta 525 (1978) 252–264.
[71] L.A. Beauge, I.M. Glynn, Nature 280 (1979) 510–512.
[72] I.M. Glynn, D.E. Richards, J. Physiol. 330 (1982) 17–43.
[73] B.I. Forbush, J. Biol. Chem. 262 (1987) 1104–1115.
[74] M. Shani, R. Goldshleger, S.J.D. Karlish, Biochim. Biophys. Acta 904 (1987) 13–21.
[75] B.I. Forbush, J. Biol. Chem. 262 (1987) 11116–11127.
[76] I.M. Gynn, J.L. Howland, D.E. Richards, J. Physiol. 368 (1985) 453–469.
[77] B.I. Forbush, in: I.M. Glynn, C. Ellory (Eds.), The Sodium Pump, Company of Biologists, Cambridge, 1985, pp. 599–611.
[78] I.M. Glynn, D.E. Richards, Y. Hara, in: I.M. Glynn, C. Ellory (Eds.), The Sodium Pump, Company of Biologists, Cambridge, 1985, pp. 589–598.
[79] D.H. MacLennan, C.J. Brandl, B. Korczak, N.M. Green, Nature 316 (1985) 696–700.
[80] S.S. Keilley, O. Meyerhoff, J. Biol. Chem. 176 (1948) 591–601.
[81] J.R. Lepock, A.M. Rodahl, C. Zhang, M.L. Heynen, B. Waters, K.H. Cheng, Biochemistry 29 (1990) 681–689.
[82] K.H. Cheng, J.R. Lepock, Biochemistry 31 (1992) 4074–4080.
[83] C. Anteneodo, A.M. Rodahl, E. Meiering, M.L. Heynen, G.A. Sennisterra, J.R. Lepock, Biochemistry 33 (1994) 12283–12290.
[84] M.P. Arendse, A.A. Aderem, D.B. McIntosh, M.C. Berman, Biochem. Biophys. Res. Commun. 101 (1981) 1426–1432.
[85] E.M. Diamond, K.B. Norton, D.B. McIntosh, M.C. Berman, J. Biol. Chem. 255 (1980) 11351–11356.
[86] A.L. Fink, Annu. Rev. Biophys. Biomol. Struct. 24 (1995) 495–522.

[87] P.R. D'Silva, A.K. Lala, J. Biol. Chem. 273 (1998) 16216–16222.
[88] J.E. Bishop, J.D. Johnson, M.C. Berman, J. Biol. Chem. 259 (1984) 15163–15171.
[89] M.C. Berman, J. Biol. Chem. 261 (1986) 16494–16501.
[90] W.P. Jencks, Adv. Enzymol. Relat. Areas Mol. Biol. 51 (1980) 4493–4497.
[91] S.C.D. Karlish, R. Goldshleger, W.D. Stein, Proc. Natl. Acad. Sci. USA 87 (1990) 4566–4570.
[92] J.M. Capasso, S. Hoving, D.M. Tal, R. Goldshleger, S.J. Karlish, J. Biol. Chem. 267 (1992) 1150–1158.
[93] E. Or, P. David, A. Shainskaya, D.M. Tal, S.J. Karlish, J. Biol. Chem. 268 (1993) 16929–16937.
[94] A. Shainskaya, V. Nesaty, S.J. Karlish, J. Biol. Chem. 273 (1998) 7311–7319.
[95] M. Kawakita, K. Yasuoka, Y. Kaziro, J. Biochem. 87 (1980) 609–617.
[96] G. Davidson, M.C. Berman, J. Biol. Chem. 262 (1987) 7041–7046.
[97] X. Yu, G. Inesi, J. Biol. Chem. 270 (1995) 4361–4367.
[98] D.B. McIntosh, D.C. Ross, P. Champeil, F. Guillain, Proc. Natl. Acad. Sci. USA 88 (1991) 6437–6441.
[99] D.C. Ross, D.B. McIntosh, J. Biol. Chem. 262 (1987) 12977–12983.
[100] D.B. McIntosh, D.G. Woolley, J. Biol. Chem. 269 (1994) 21587–21595.
[101] G.W. Gould, J. Colyer, J.M. East, A.G. Lee, J. Biol. Chem. 262 (1987) 7676–7679.
[102] T. Suzuki, M. Kawakita, J. Biochem. 114 (1993) 203–209.
[103] L. De Meis, J. Biol. Chem. 266 (1991) 5736–5742.
[104] H. Wolosker, L. De Meis, Biosci. Rep. 15 (1995) 365–376.
[105] E.W. Alves, L. De Meis, Eur. J. Biochem. 166 (1987) 647–651.
[106] L. De Meis, V.A. Suzano, J. Biol. Chem. 269 (1994) 14525–14529.
[107] U. Gerdes, J.V. Moller, Biochim. Biophys. Acta 734 (1983) 191–200.
[108] A. Galina, L. De Meis, J. Biol. Chem. 266 (1991) 17978–17982.
[109] G. Wang, D.S. Perlin, Arch. Biochem. Biophys. 344 (1997) 309–315.
[110] P. Soteropoulos, D.S. Perlin, J. Biol. Chem. 273 (1998) 26426–26431.
[111] G. Wang, M.J. Tamas, M.J. Hall, A. Pascual-Ahuir, D.S. Perlin, J. Biol. Chem. 271 (1996) 25438–25445.
[112] P. Soteropoulus, A. Valiakhmetov, R. Kashiwazaki, D.S. Perlin, J. Biol. Chem. (2001), in press.
[113] K. Venema, M.G. Palmgren, J. Biol. Chem. 270 (1995) 19659–19667.
[114] L. Baunsgaard, K. Venema, K.B. Axelsen, J.M. Villalba, A. Welling, B. Wollenweber, M.G. Palmgren, Plant J. 10 (1996) 451–458.
[115] M.J. Buch-Pedersen, K. Venema, R. Serrano, M.G. Palmgren, J. Biol. Chem. 275 (2000) 39167–39173.
[116] J.P. Andersen, Biosci. Rep. 15 (1995) 243–261.
[117] J.P. Andersen, T. Sorenson, Biochim. Biophys. Acta 1275 (1996) 118–122.
[118] J.P. Andersen, B. Vilsen, FEBS Lett. 359 (1995) 101–106.
[119] J.P. Andersen, J. Biol. Chem. 270 (1995) 908–914.
[120] W. Hasselbach, Prog. Biophys. Biophys. Chem. 14 (1964) 167–222.
[121] A. Martonosi, A. Feretos, J. Biol. Chem. 239 (1964) 659–668.
[122] G. Inesi, M. Kurzmack, S. Verjowski-Almeida, Ann. N.Y. Acad. Sci. 307 (1978) 224–227.
[123] L. De Meis, M.G.C. Carvalho, Biochemistry 13 (1974) 5032–5038.
[124] G. Inesi, R. Nakamoto, L. Hymel, S. Fleischer, J. Biol. Chem. 258 (1983) 14804–14809.
[125] G.W. Gould, J.M. McWhirter, A.G. Lee, Biochim. Biophys. Acta 904 (1987) 45–54.
[126] L. De Meis, The Sarcoplasmic Reticulum: Transport and Energy Transduction, John Wiley and Sons, New York, 1981.
[127] J.M. McWhirter, G.W. Gould, J.M. East, A.G. Lee, Biochem. J. 245 (1987) 713–722.
[128] P.D. Boyer, L. De Meis, M.G.C. Carvalho, D.D. Hackney, Biochemistry 16 (1977) 136–140.
[129] N. Yamamoto, M. Kasai, J. Biochem. (Tokyo) 92 (1982) 485–496.
[130] G. Meissner, E. Darling, J. Yvelette, Biochemistry 25 (1986) 236–244.
[131] B.A. Suarez-Isla, C. Orezco, P.F. Heller, J.P. Frohlich, Proc. Natl. Acad. Sci. USA 83 (1986) 7741–7745.
[132] V. Gerdes, J.V. Moller, Biochim. Biophys. Acta 734 (1983) 191–200.
[133] J.M. McWhirtir, G.W. Gould, J.M. East, A.G. Lee, Biochem. J. 245 (1987) 713–722.
[134] C. Tanford, J.A. Reynolds, E.A. Johnson, Proc. Natl. Acad. Sci. USA 84 (1987) 7094–7098.
[135] Y. Kakamura, M. Kurzmack, G. Inesi, J. Biol. Chem. 261 (1986) 3090–3097.
[136] D.B. McIntosh, P.D. Boyer, Biochemistry 22 (1983) 2867–2875.
[137] N. Stahl, W.P. Jencks, Biochemistry 23 (1984) 5889–5892.
[138] M. Shigekawa, A.A. Akowitz, J. Biol. Chem. 254 (1979) 4726–4730.
[139] B. Rossi, F. de Assis Leone, C. Gache, M. Lazdunski, J. Biol. Chem. 254 (1979) 2302–2307.
[140] M. Kushmerick, Hand. Physiol. 10 (1983) 189–236.
[141] D. Levy, A. Gulik, A. Bluzat, J.L. Rigaud, Biochim. Biophys. Acta 1107 (1992) 283–298.
[142] J.A. Holgiun, Arch. Biochem. Biophys. 251 (1986) 9–16.
[143] P. Mermier, W. Hasselbach, Eur. J. Biochem. 69 (1976) 79–86.
[144] M.C. Berman, S.B. King, Biochim. Biophys. Acta 1029 (1990) 235–240.
[145] T. Fujimori, W.P. Jencks, J. Biol. Chem. 267 (1992) 18466–18474.
[146] T. Fujimori, W.P. Jencks, J. Biol. Chem. 267 (1992) 18475–18487.

[147] S. Orlowski, P. Champeil, FEBS Lett. 328 (1993) 296–300.
[148] H. Guimaraes-Motta, M.P. Sande-Lemos, L. De Meis, J. Biol. Chem. 259 (1984) 8699–8705.
[149] G. Inesi, R. Nakamoto, L. Hymel, S. Fleischer, J. Biol. Chem. 258 (1983) 14804–14809.
[150] X. Yu, G. Inesi, FEBS Lett. 328 (1993) 301–304.
[151] X. Yu, S. Carroll, J.L. Rigaud, G. Inesi, Biophys. J. 64 (1993) 1232–1242.
[152] K.A. Dalton, J.M. East, S. Mall, S. Oliver, A.P. Starling, A.G. Lee, Biochem. J. 329 (1998) 637–646.
[153] K.A. Dalton, J.D. Pilot, S. Mall, J.M. East, A.G. Lee, Biochem. J. 342 (1999) 431–438.
[154] J.L. Rigaud, B. Pitard, D. Levy, Biochim. Biophys. Acta 123 (1995) 223–246.
[155] Y.H. Lau, A.H. Caswell, J. Brunschig, R.J. Baerwald, M. Garcia, J. Biol. Chem. 254 (1979) 540–546.
[156] H. Milting, L.M.G. Heilmeyer, R. Thieleczek, FEBS Lett. 345 (1994) 211–218.
[157] F. Michelangeli, S. Orlowski, P. Champeil, E.A. Grimes, J.M. East, A.G. Lee, Biochemistry 29 (1990) 8307–8312.
[158] C. Toyoshima, H. Sasabe, D.L. Stokes, Nature 362 (1993) 467–471.
[159] D.B. McIntosh, G.A. Davidson, Biochemistry 23 (1984) 1959–1965.
[160] S. Meltzer, M.C. Berman, Anal. Biochem. 138 (1984) 458–464.
[161] S. Meltzer, M.C. Berman, J. Biol. Chem. 259 (1984) 4244–4253.
[162] A.L. Vianna, Biochim. Biophys. Acta 410 (1975) 389–406.
[163] R. The, W. Hasselbach, Eur. J. Biochem. 28 (1972) 357–362.
[164] K.E. Neet, N.M. Green, Arch. Biochem. Biophys. 178 (1977) 588–597.
[165] P.F. Duggan, J. Biol. Chem. 252 (1977) 1620–1627.
[166] C.A. Tate, A. Chu, J. McMillan-Wood, W.B. Van Winkle, M.L. Entman, J. Biol. Chem. 256 (1981) 2934–2939.
[167] G. Inesi, M. Millman, S. Eletr, J. Mol. Biol. 81 (1973) 483–504.
[168] G. Davis, G. Inesi, T. Gulik-Krzynicki, Biochemistry 15 (1976) 1271–1276.
[169] J.M. Van der Kooi, A. Martonosi, Arch. Biochem. Biophys. 147 (1971) 632–646.
[170] V.C.K. Chiu, D.H. Haynes, Biophys. J. 18 (1977) 3–22.
[171] V.C.K. Chiu, D.H. Haynes, J. Membr. Biol. 56 (1980) 203–218.
[172] M.M. Sorenson, J. Biol. Chem. 258 (1983) 7684–7690.
[173] G. Meissner, D. McKinley, J. Membr. Biol. 30 (1976) 79–98.
[174] Y.H. Lau, Biochim. Biophys. Acta 730 (1983) 276–284.
[175] J.J. Feher, F.N. Briggs, J. Biol. Chem. 257 (1982) 10191–10199.
[176] H. Takenaka, P.N. Adler, A.M. Katz, J. Biol. Chem. 257 (1982) 12649–12656.
[177] G.E. Taffet, C.A. Tate, Arch. Biochem. Biophys. 299 (1992) 287–294.
[178] A. Pucell, A. Martonosi, J. Biol. Chem. 246 (1971) 3389–3397.
[179] M. Makinose, R. The, Biochem. Z. 343 (1965) 383–389.
[180] W. Hasselbach, Biochim. Biophys. Acta 515 (1978) 23–53.
[181] M. Fortea, F. Soler, F. Fernandez-Belda, J. Biol. Chem. 275 (2000) 12521–12529.
[182] F. Soler, F. Pleuge-Tellechea, I. Fortes, F. Fernandez-Belda, Biochemistry 37 (1998) 4266–4274.
[183] P. Champeil, F. Guillain, Biochemistry 25 (1986) 7623–7633.
[184] S. Wakabayashi, T. Ogurusu, M. Shigekawa, J. Biol. Chem. 261 (1986) 9762–9769.
[185] Y. Takakuwa, T. Kanazawa, J. Biol. Chem. 256 (1981) 2696–2700.
[186] F. Soler, J.A. Teruel, F.J. Fernandez-Belda, C. Gomez-Fernandez, Eur. J. Biochem. 192 (1990) 347–354.
[187] P.J. Garrahan, I.M. Glynn, J. Physiol. (Lond.) 192 (1967) 159–174.
[188] P.J. Garrahan, I.M. Glynn, J. Physiol. (Lond.) 192 (1967) 217–235.
[189] I.M. Glynn, J.F. Hoffman, J. Physiol. (Lond.) 218 (1971) 239–256.
[190] J.D. Cavieres, I.M. Glynn, J. Physiol. (Lond.) 297 (1979) 637–645.
[191] B.G. Kennedy, G. Lunn, J.F. Hoffman, J. Gen. Physiol. 87 (1986) 47–72.
[192] V.L. Lew, M.A. Hardy, J.C. Elloy, Biochim. Biophys. Acta 232 (1973) 251–266.
[193] I.M. Glynn, S.J.D. Karlish, J. Physiol. (Lond.) 256 (1976) 465–496.
[194] K.H. Lee, R. Blostein, Nature 285 (1980) 338–339.
[195] R. Blostein, J. Biol. Chem. 258 (1983) 7948–7953.
[196] S. Yoda, A. Yoda, J. Biol. Chem. 263 (1986) 1147–1152.
[197] S. Yoda, A. Yoda, J. Biol. Chem. 261 (1987) 103–109.
[198] A. Yoda, S. Yoda, J. Biol. Chem. 262 (1987) 110–115.
[199] F. Cornelius, J.C. Skou, Biochim. Biophys. Acta 818 (1985) 211–221.
[200] R. Goldshleger, Y. Shahak, S.J.D. Karlish, J. Membr. Biol. 113 (1990) 139–154.
[201] S.J.D. Karlish, W.D. Stein, J. Physiol. (Lond.) 359 (1985) 119–149.
[202] S.J.D. Karlish, Methods Enzymol. 156 (1988) 179–188.
[203] D.F.S. Rolfe, G.C. Brown, Physiol. Rev. 77 (1997) 731–758.
[204] T. Clausen, C. Van Hardeveld, M.E. Everts, Physiol. Rev. 71 (1991) 733–774.
[205] E. Homsher, Annu. Rev. Physiol. 49 (1987) 672–690.
[206] A. Chinet, T. Clausen, L. Girardier, J. Physiol. (Lond.) 265 (1977) 43–61.
[207] A.L. Hodgkin, P. Horowicz, J. Physiol. (Lond.) 148 (1959) 127–160.
[208] C.D. Nobes, G.C. Brown, P.N. Olive, M.D. Brand, J. Biol. Chem. 265 (1990) 12903–12909.
[209] M. Erecinska, I.A. Silver, J. Cereb. Blood Flow Metab. 9 (1989) 2–19.
[210] B.A. Block, Annu. Rev. Physiol. 56 (1994) 535–577.

[211] L. De Meis, M.L. Bianconi, V.A. Suzano, FEBS Lett. 406 (1997) 201–204.
[212] L. De Meis, Biochem. Biophys. Res. Commun. 243 (1998) 598–600.
[213] L. De Meis, Biochem. Biophys. Res. Commun. 276 (2000) 35–39.
[214] B.A. Block, C. Franzini-Armstrong, J. Cell Biol. 107 (1988) 1099–1112.
[215] B.A. Block, J. Morphol. 190 (1986) 169–189.
[216] B.A. Block, Annu. Rev. Physiol. 56 (1994) 535–577.
[217] N. Narayanan, D.L. Jones, A. Xu, J.C. Yu, Am. J. Physiol. 271 (1996) C1032–C1040.
[218] R.I. Viner, D.A. Ferrington, T.D. Williams, D.J. Bigelow, C. Schoneich, Biochem. J. 340 (1999) 657–659.
[219] D.A. Ferrington, T.E. Jones, Z. Qin, M. Miller-Schlyer, D.J. Bigelow, Biochim. Biophys. Acta 1330 (1997) 233–247.
[220] J.T. Parsons, S.B. Churn, R.J. DeLorenzo, Brain Res. 834 (1999) 32–41.
[221] D.L. Jones, N. Narayanan, Am. J. Physiol. 274 (1998) H98–H105.
[222] M.M. Bersohn, J. Mol. Cell. Cardiol. 27 (1995) 1483–1489.
[223] L.P. Faucheux, G. Stolovitsky, A. Libchaber, Phys. Rev. E 51 (1995) 5239–5250.